

UNSYMMETRICAL LARGE DEFLECTIONS  
OF AN ANNULAR PLATE

by

William Edmund Alzheimer

Thesis submitted to the Graduate Faculty of the  
Virginia Polytechnic Institute  
in candidacy for the degree of

DOCTOR OF PHILOSOPHY

in

ENGINEERING MECHANICS

APPROVED:

\_\_\_\_\_  
Chairman, R. T. Davis

\_\_\_\_\_  
G. A. Gray

\_\_\_\_\_  
G. B. Ling

\_\_\_\_\_  
A. A. Pap

\_\_\_\_\_  
G. W. Swift

\_\_\_\_\_  
D. H. Pletta, Head of Department

August, 1966

Blacksburg, Virginia

TABLE OF CONTENTS

<u>Chapter</u>	<u>Page</u>
LIST OF ILLUSTRATIONS .....	4
NOMENCLATURE .....	5
I. INTRODUCTION .....	7
II. REVIEW OF LITERATURE .....	11
III. FORMULATION OF THE PROBLEM .....	14
A. Governing Equations .....	14
B. Boundary Conditions .....	21
IV. SOLUTION TO THE PROBLEM .....	24
A. First Approximation .....	25
B. Second Approximation .....	27
C. Discussion .....	43
V. EXPERIMENTAL INVESTIGATION .....	57
A. Experimental Apparatus .....	57
B. Comparison Between Experiment and the Iteration Solution .....	59
VI. CONCENTRATED MOMENT .....	66
A. Solution by Iteration .....	66
B. Discussion .....	71
VII. EXTENSION OF THE PROBLEM .....	74
A. Series Truncation .....	74
B. Large Initial Prestress .....	77
VIII. ACKNOWLEDGMENTS .....	86

<u>Chapter</u>	<u>Page</u>
IX. BIBLIOGRAPHY .....	87
X. VITA .....	91
APPENDIX A. Derivation of von Karman Equations from Equations of Elasticity .....	92

LIST OF ILLUSTRATIONS

<u>Figure</u>	<u>Page</u>
1. Coordinate system and geometry .....	15
2. Displacements and stress resultants .....	16
3. Lateral displacement along radial line normal to axis of rotation .....	47
4. Radial displacement along radial line normal to axis of rotation .....	48
5. Maximum tangential displacement .....	49
6. Applied moment-angle of rotation relationships .....	50
7. Effect of thickness on applied moment ( $\beta = 0.4$ ) .....	51
8. Effect of thickness on applied moment ( $\beta = 0.7$ ) .....	52
9. Maximum radial bending stress .....	53
10. Maximum stresses .....	54
11. Variation of radial stresses along the line $\theta = 0$ ....	55
12. Maximum total radial stress ( $\beta = 0.4$ ) .....	56
13. Experimental apparatus .....	61
14. Experimental apparatus .....	62
15. Experimental moment-rotation curve .....	63
16. Experimental maximum total radial strain .....	64
17. Experimental bending and membrane radial strains .....	65
18. Maximum lateral displacement for concentrated moment .....	73

NOMENCLATURE

$r, \theta, z$	cylindrical polar coordinates
$a, b$	outer and inner radius respectively
$\rho$	dimensionless radial coordinate ( $r/a$ )
$\beta$	dimensionless inner radius ( $b/a$ )
$h$	plate thickness
$\lambda$	outer radius - thickness ratio ( $a/h$ )
$\nu$	Poisson's ratio
$E$	Young's modulus
$D$	flexural rigidity of plate ( $Eh^3/12(1-\nu^2)$ )
$u, v, w$	displacements in $r, \theta, z$ directions
$U, V, W$	dimensionless displacements ( $u/a, v/a, w/a$ )
$n_r, n_\theta, n_{r\theta}$	in-plane stress resultants
$N_r, N_\theta, N_{r\theta}$	dimensionless in-plane stress resultants $(n_r \frac{a^2}{D}, n_\theta \frac{a^2}{D}, n_{r\theta} \frac{a^2}{D})$
$m_r, m_\theta, m_{r\theta}$	moment resultants
$M_r, M_\theta, M_{r\theta}$	dimensionless moment resultants ( $m_r \frac{a}{D}, m_\theta \frac{a}{D}, m_{r\theta} \frac{a}{D}$ )
$q_r, q_\theta$	transverse shearing stress resultants
$Q_r, Q_\theta$	dimensionless transverse shearing stress resultants $(q_r \frac{a^2}{D}, q_\theta \frac{a^2}{D})$

- $\sigma_r', \sigma_\theta'$  dimensionless membrane stresses (  $\frac{n_r}{hE}, \frac{n_\theta}{hE}$  )
- $\sigma_r'', \sigma_\theta''$  dimensionless bending stresses (  $\frac{6m_r}{Eh^2}, \frac{6m_\theta}{Eh^2}$  )  
at outer surface
- $\sigma_{r1}'', \sigma_{\theta 1}''$  dimensionless bending stresses at outer surface from  
linear theory
- $\alpha$  angle of rotation of inner inclusion (radians)
- $m$  moment applied to inclusion
- $M$  dimensionless moment applied to inclusion (  $\frac{m}{D}$  )
- $\varphi$  stress function

$\nabla^4$  biharmonic operator (cylindrical coordinates)

$$\left( \frac{\partial^2}{\partial \rho^2} + \frac{1}{\rho} \frac{\partial}{\partial \rho} + \frac{1}{\rho^2} \frac{\partial^2}{\partial \theta^2} \right) \left( \frac{\partial^2}{\partial \rho^2} + \frac{1}{\rho} \frac{\partial}{\partial \rho} + \frac{1}{\rho^2} \frac{\partial^2}{\partial \theta^2} \right)$$

$L(W, \varphi)$  operator

$$\frac{\partial^2 W}{\partial \rho^2} \left( \frac{1}{\rho} \frac{\partial \varphi}{\partial \rho} + \frac{1}{\rho^2} \frac{\partial^2 \varphi}{\partial \theta^2} \right) + \frac{\partial^2 \varphi}{\partial \rho^2} \left( \frac{1}{\rho} \frac{\partial W}{\partial \rho} + \frac{1}{\rho^2} \frac{\partial^2 W}{\partial \theta^2} \right)$$

$$- 2 \frac{\partial}{\partial \rho} \left( \frac{1}{\rho} \frac{\partial W}{\partial \theta} \right) \frac{\partial}{\partial \rho} \left( \frac{1}{\rho} \frac{\partial \varphi}{\partial \theta} \right)$$

Plus miscellaneous symbols defined in the text.

## I. INTRODUCTION

Classical linear thin plate theory, which neglects the straining of the middle surface of the plate, is known to give satisfactory results as long as the deflections are small compared to the thickness of the plate. In cases where the deflections are of the same order of magnitude as the thickness, the stretching of the middle surface is no longer negligible and should be included in the analysis. The in-plane stresses caused by stretching the middle surface produce a stiffening effect on the plate, which leads to a reduction in lateral displacement. The coupling effects between the in-plane stresses and the lateral displacement, for cases where the displacements are two or three times as large as the thickness, are included in the two, coupled, nonlinear von Karman thin plate equations.

The object of this investigation is to obtain a solution to the von Karman equations for a thin annular plate, which is fixed at the outer boundary and which has a central rigid plug that is rotated about its diameter out of the plane of the plate. Two earlier publications dealt with the linear, small deflection solution to this problem. In 1930, H. Reissner (13) presented the analytical solution for small deflections and in 1932, Roark (14) published experimental results for the same problem. Roark became involved with this problem

during an investigation of a drum-head which had developed cracks during service.

Solutions to the von Karman equations exist in the literature for annular plates with certain axisymmetrical loading conditions. However, it appears that the only previous application of the von Karman equations to unsymmetrical deformations was in a split-ring problem presented by E. Reissner (10), in which the in-plane stresses were axisymmetric but the lateral displacement varied linearly with the azimuthal coordinate.

Probably the most successful method used thus far in obtaining solutions to the von Karman equations has been the straight-forward perturbation procedure. In this investigation a systematic mathematical iteration procedure, which is equivalent to the straight-forward perturbation method, is used. The iteration procedure has the advantage that the form of solution automatically emerges during the iteration, whereas in the straight-forward perturbation method the correct form of the solution must be assumed initially in a series expansion in the perturbation parameter.

To begin the iteration procedure the correct first approximation must be known, and in this case H. Reissner's (13) small deflection solution is used as a first approximation to the "large deflection" lateral displacement. The nonlinear part of one of the von Karman



equations is evaluated using the first approximation to the lateral displacement, and a linear, fourth order partial differential equation for the stress function is obtained. The particular solution to the stress function equation leads to multi-valued in-plane displacements, which are eliminated by proper selection of the homogeneous solution. The boundary conditions for the stress function are written in terms of the in-plane displacements. Wherever trigonometric functions of the small angle of rotation of the rigid hub appear, they are expanded in a power series of the angle and terms of higher order than the second power are neglected.

By using the resulting stress function and the lateral displacement from linear theory to evaluate the nonlinear part of the second von Karman equations, a linear fourth order partial differential equation for the second approximation to the lateral displacement is obtained. Again the boundary conditions are expressed in a power series in the rotation angle and terms of higher order than the third power are neglected. The solution for the second approximation to the lateral displacement contains the first and third powers of the rotation angle, where the part containing the first power is the Reissner solution and the part containing the third power is a correction term reflecting a reduction in lateral displacement caused by the in-plane stresses. Thus by neglecting the third power of the

small angle of rotation, the large deflection solution reduces to Reissner's small deflection solution.

The iteration is terminated after obtaining the second approximation because the algebra becomes excessive; however, it can be continued to obtain higher approximations for thin plates. By taking appropriate derivatives of the stress function and lateral displacement, expressions for the membrane and bending stresses are obtained.

Because the algebraic expressions developed are quite lengthy, numerical values for stresses and displacements in typical plates are obtained with a digital computer. The results are shown to agree very well with experimental data obtained during this investigation with the help of Liberty and Collier (8). As a limiting case, the solution is obtained for a concentrated moment applied at the center of a clamped circular plate.

## II. REVIEW OF LITERATURE

Although von Karman presented his large deflection plate equations in 1910, very few solutions were obtained until the late 1940's. A series solution presented by Way (22) in 1934 for a circular plate with uniform loading was the earliest successful attempt. In 1947 Chien (1) solved the same problem using a straight-forward perturbation method and found this method eliminated much of the tedious numerical work encountered by Way. The results of both methods agreed very well with experimental work done by Way in conjunction with his analytical solution.

Since 1947 several investigators have used perturbation techniques similar to Chien's to solve the von Karman equations for plates of various geometries and including such effects as anisotropy, variable thickness, etc. Only the literature pertaining to large deflections of annular plates will be reviewed here, but the reader is referred to references (15) and (21) for a comprehensive bibliography of investigations of large deflections for other geometries.

In 1954, E. Reissner (10) presented a closed form solution to the von Karman equations for a circular ring sector under the action of two equal and opposite forces and a twisting moment, both applied along the centroidal axis normal to the plane of the sector. Reissner's paper is the only known work on unsymmetrical deformations

of annular plates prior to this investigation. However, in Reissner's paper the lateral displacement was a linear function of the azimuthal coordinate and the in-plane displacements were functions of only the radial coordinate, whereas in this investigation all three displacements are functions of both coordinates.

In 1958 Wempner and Schmidt (23) presented a series solution, similar to Way's, to the von Karman plate equations for an annular plate, simply supported at the outer edge and loaded along the free inner boundary by axisymmetric edge loads. In 1963 Koehli and Evan-Iwanowski (7) presented a similar solution for an annular plate, fixed at the inner boundary and loaded along the free outer boundary by axisymmetric edge loads. Since they were interested in the practical application of clutching devices, Koehli and Evan-Iwanowski also included the rotary inertia loading.

In 1964 Tamate and Abe (17) obtained a numerical solution by finite difference techniques for an annular plate, whose outer boundary is clamped and inner boundary free. They considered only a uniform pressure loading.

The only other known papers dealing with large deflections of annular plates consider the same geometry as in this investigation, but only the axisymmetric case of a concentrated force applied at the center of the rigid inclusion is treated. In 1964 Hart and Evans (6) considered the above problem and used a perturbation method to solve

the von Karman equations. They also obtained a numerical solution to a more exact set of large deflection plate equations given by E. Reissner (11), and compared the two solutions. They found the results of the von Karman equations compared very well with those from the more exact Reissner equations except for very large loads (loads giving stresses well in excess of the elastic limit). They also found the von Karman equations tend to underestimate the membrane stresses. In 1965 Hamada and Seguchi (5) obtained a numerical solution to the von Karman equations for the same problem, and also for the outer boundary conditions of simple supports and hinges. They obtained experimental results for the case of both edges clamped and found good agreement between experiment and the numerical solution.

### III. FORMULATION OF THE PROBLEM

The von Karman thin plate equations are based upon the following assumptions:

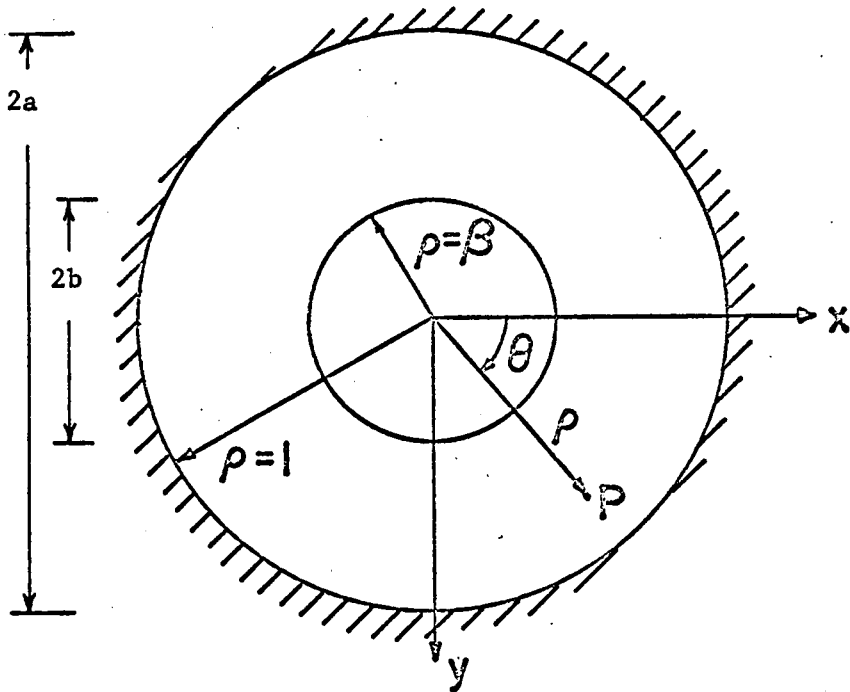
- (1) strains vary linearly within the plate thickness (lines normal to the middle surface remain normal to it).
- (2) stresses on surfaces parallel to the middle surface can be neglected.
- (3) the slope of the deflected surface and the strain components are small.
- (4) the in-plane displacements ( $u$  and  $v$ ) are small compared to the lateral displacement ( $w$ ), so that only those non-linear terms depending on the lateral displacement need be retained in the strain displacement relations.

These assumptions differ from those of classical linear plate theory by retaining part of the nonlinear terms in the strain displacement relations and by not requiring the middle surface to remain undeformed.

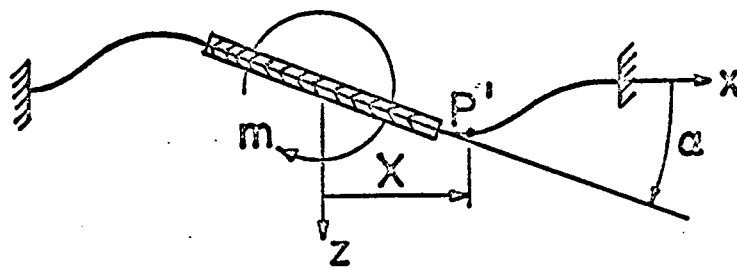
In this chapter the von Karman equations are derived in polar coordinates and the boundary conditions for the annular plate are developed.

#### A. Governing Equations.

The governing equations are obtained in this section by considering the equilibrium of a deformed element of the plate as shown in Figure 2.

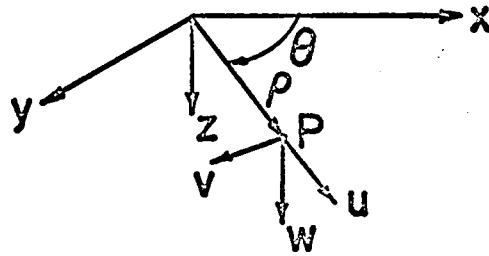


TOP VIEW UNDEFORMED PLATE

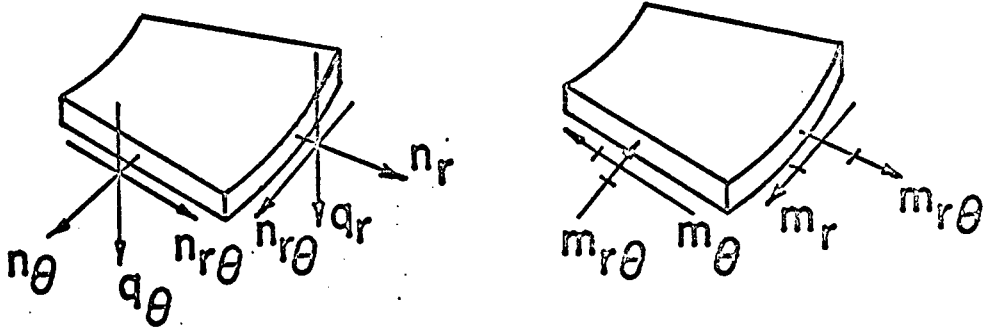


DEFORMED CONFIGURATION

FIGURE 1. Coordinate system and geometry



### DISPLACEMENTS



### RESULTANTS

FIGURE 2. Displacements and stress resultants



The equations of equilibrium are found by projecting the forces acting on the deformed element onto the undeformed polar coordinate axes. For a plate of constant thickness which has no body or surface loading, the equilibrium equations (dimensionless quantities are defined in Nomenclature) in the  $\rho$  and  $\theta$  directions are:

$$\frac{\partial N_r}{\partial \rho} + \frac{1}{\rho} \frac{\partial N_{r\theta}}{\partial \theta} + \frac{1}{\rho} (N_r - N_\theta) = 0 \quad (1)$$

$$\frac{1}{\rho} \frac{\partial N_\theta}{\partial \theta} + \frac{\partial N_{r\theta}}{\partial \rho} + 2 \frac{N_{r\theta}}{\rho} = 0 \quad (2)$$

Equations (1) and (2) are identically satisfied by introducing the following stress function  $\varphi$ :

$$N_r = \frac{1}{\rho} \frac{\partial \varphi}{\partial \rho} + \frac{1}{\rho^2} \frac{\partial^2 \varphi}{\partial \theta^2} \quad (3)$$

$$N_\theta = \frac{\partial^2 \varphi}{\partial \rho^2} \quad (4)$$

$$N_{r\theta} = - \frac{\partial}{\partial \rho} \left( \frac{1}{\rho} \frac{\partial \varphi}{\partial \theta} \right) \quad (5)$$

Using Hooke's law, equations (3), (4) and (5) can be written in terms of the normal strains  $\epsilon_r$  and  $\epsilon_\theta$  and the shearing strain  $\gamma_{r\theta}$  as follows:

$$\epsilon_r = \frac{\lambda^{-2}}{12(1-\nu^2)} \left[ \frac{1}{\rho} \frac{\partial \phi}{\partial \rho} + \frac{1}{\rho^2} \frac{\partial^2 \phi}{\partial \theta^2} - \nu \frac{\partial^2 \phi}{\partial \rho^2} \right] \quad (6)$$

$$\epsilon_\theta = \frac{\lambda^{-2}}{12(1-\nu^2)} \left[ \frac{\partial^2 \phi}{\partial \rho^2} - \nu \left( \frac{1}{\rho} \frac{\partial \phi}{\partial \rho} + \frac{1}{\rho^2} \frac{\partial^2 \phi}{\partial \theta^2} \right) \right] \quad (7)$$

$$\gamma_{r\theta} = - \frac{\lambda^{-2}}{6(1-\nu)} \frac{\partial}{\partial \rho} \left( \frac{1}{\rho} \frac{\partial \phi}{\partial \theta} \right) \quad (8)$$

In polar coordinates, the middle surface strain-displacement relations which are consistent with the von Karman theory are:

$$\epsilon_r = \frac{\partial U}{\partial \rho} + \frac{1}{2} \left( \frac{\partial W}{\partial \rho} \right)^2 \quad (9)$$

$$\epsilon_\theta = \frac{U}{\rho} + \frac{1}{\rho} \frac{\partial V}{\partial \theta} + \frac{1}{2} \left( \frac{1}{\rho} \frac{\partial W}{\partial \theta} \right)^2 \quad (10)$$

$$\gamma_{r\theta} = \frac{1}{\rho} \frac{\partial U}{\partial \theta} - \frac{V}{\rho} + \frac{\partial V}{\partial \rho} + \frac{1}{\rho} \frac{\partial W}{\partial \rho} \frac{\partial W}{\partial \theta} \quad (11)$$

where, according to assumption (4) stated at the beginning of this chapter, nonlinear terms involving derivatives of W are retained, but nonlinear terms involving derivatives of the in-plane displacements (for example  $(\frac{\partial U}{\partial \rho})^2$ ) have been neglected. It will be apparent from the solutions given in the next chapter, that derivatives of the

in-plane displacements are of higher order than those of the lateral displacement and thus can be neglected.

By taking two derivatives of equations (9), (10) and (11) and combining the resulting expressions, the following compatibility equation is found:

$$\begin{aligned} \frac{\partial^2 \epsilon_{\theta}}{\partial \rho^2} + \frac{1}{\rho} \frac{\partial^2 \epsilon_r}{\partial \theta^2} + \frac{2}{\rho} \frac{\partial \epsilon_{\theta}}{\partial \rho} - \frac{1}{\rho} \frac{\partial \epsilon_r}{\partial \theta} - \frac{1}{\rho} \frac{\partial^2 \gamma_{r\theta}}{\partial \rho \partial \theta} \\ - \frac{1}{\rho} \frac{\partial \gamma_{r\theta}}{\partial \theta} = - \frac{1}{2} L(W, W) \end{aligned} \quad (12)$$

where  $L(W, W)$  is obtained from  $L(W, \varphi)$  by simply replacing  $\varphi$  with  $W$  (see Nomenclature). Combining equations (6), (7) and (8) with equation (12) results in the following equation:

$$\nabla^4 \varphi = - 6 (1 - \nu^2) \lambda^2 L(W, W) \quad (13)$$

The equilibrium equation in the transverse direction is:

$$\begin{aligned} \frac{\partial Q_r}{\partial \rho} + \frac{1}{\rho} \frac{\partial Q_{\theta}}{\partial \theta} + \frac{Q_r}{\rho} = - \left[ N_r \frac{\partial^2 W}{\partial \rho^2} + N_{\theta} \left( \frac{1}{\rho} \frac{\partial W}{\partial \rho} + \frac{1}{\rho^2} \frac{\partial^2 W}{\partial \theta^2} \right) \right. \\ \left. + 2 N_{r\theta} \frac{\partial}{\partial \rho} \left( \frac{1}{\rho} \frac{\partial W}{\partial \theta} \right) \right] \end{aligned} \quad (14)$$

and summation of moments about the  $\rho$  and  $\theta$  axes gives:

$$\frac{1}{\rho} \frac{\partial M_{\theta}}{\partial \theta} - \frac{\partial M_{r\theta}}{\partial \rho} - \frac{2}{\rho} M_{r\theta} = Q_{\theta} \quad (15)$$

$$\frac{\partial M_r}{\partial \rho} - \frac{1}{\rho} \frac{\partial M_{r\theta}}{\partial \theta} = Q_r \quad (16)$$

By substituting for  $Q_r$  and  $Q_{\theta}$  from equations (15) and (16) and using the moment-curvature relations:

$$M_r = - \left[ \frac{\partial^2 W}{\partial \rho^2} + \nu \left( \frac{1}{\rho} \frac{\partial W}{\partial \rho} + \frac{1}{\rho^2} \frac{\partial^2 W}{\partial \theta^2} \right) \right] \quad (17)$$

$$M_{\theta} = - \left[ \frac{1}{\rho} \frac{\partial W}{\partial \rho} + \frac{1}{\rho^2} \frac{\partial^2 W}{\partial \theta^2} + \nu \frac{\partial^2 W}{\partial \rho^2} \right] \quad (18)$$

$$M_{r\theta} = (1-\nu) \frac{\partial}{\partial \rho} \left( \frac{1}{\rho} \frac{\partial W}{\partial \theta} \right) \quad (19)$$

equation (14) is reduced to:

$$\nabla^4 W = L(W, \varphi) \quad (20)$$

Equations (13) and (20) are the two, coupled, nonlinear von Karman plate equations. These equations are also derived from the equations of finite elasticity in Appendix A.

B. Boundary Conditions.

The von Karman equations as derived here are based on the Lagrangian description and therefore the boundary conditions should be written in terms of the undeformed coordinates. To determine the displacements of points on the inner boundary of the plate, consider the arbitrary point P in Figure 1 to be located in the central rigid plug. The coordinates of P in the undeformed position are (x, y, 0) in rectangular cartesian coordinates and ( $\rho$ ,  $\theta$ , 0) in polar coordinates. Rotating the rigid hub an angle  $\alpha$  about the y axis causes P to move to position P' which has coordinates (X, y, w).

The displacements of P measured from the undeformed position are:

$$w = X \tan \alpha \quad (21)$$

$$u = - (x - X) \cos \theta \quad (22)$$

$$v = (x - X) \sin \theta \quad (23)$$

where:

$$x = a \rho \cos \theta \quad (24)$$

$$X = a \rho \cos \theta \cos \alpha \quad (25)$$

To evaluate ( $\frac{\partial w}{\partial \rho}$ ) in the rigid hub, it is convenient to use the chain rule for partial differentiation:

$$\frac{\partial w}{\partial \rho} = \frac{\partial w}{\partial X} \frac{\partial X}{\partial \rho} + \frac{\partial w}{\partial y} \frac{\partial y}{\partial \rho} \quad (26)$$

where from equation (21):

$$\frac{\partial w}{\partial X} = \tan \alpha \quad (27)$$

and since the rigid hub is rotated about the y axis

$$\frac{\partial w}{\partial y} = 0 \quad (28)$$

Using equations (25), (26), (27) and (28) the following expression is obtained:

$$\frac{\partial w}{\partial \rho} = a \cos \theta \sin \alpha \quad (29)$$

Equations (21), (22), (23) and (29) give the displacements and rotation of all points in the rigid hub, and evaluating these at the inner boundary of the plate ( $\rho = \beta$ ,  $x = b \cos \theta$ ,  $X = b \cos \theta \cos \alpha$ ) the inner boundary conditions become:

$$w = b \cos \theta \sin \alpha \quad (30)$$

$$\frac{\partial w}{\partial \rho} = a \cos \theta \sin \alpha \quad (31)$$

$$u = -b \cos^2 \theta (1 - \cos \alpha) \quad (32)$$

$$v = b \cos \theta \sin \theta (1 - \cos \alpha) \quad (33)$$

Expressing the trigonometric functions of the small angle of rotation  $\alpha$  in a power series and keeping only terms to order  $\alpha^3$

(since this is as far as the iteration procedure is pursued), the inner boundary conditions (dimensionless form) for the plate become:

$$W = \beta \left( \alpha - \frac{\alpha^3}{6} + \dots \right) \cos \theta \quad (34)$$

$$\frac{\partial W}{\partial \rho} = \left( \alpha - \frac{\alpha^3}{6} + \dots \right) \cos \theta \quad (35)$$

$$U = -\beta \left( \frac{\alpha^2}{4} + \dots \right) (1 + \cos 2\theta) \quad (36)$$

$$V = \beta \left( \frac{\alpha^2}{4} + \dots \right) \sin 2\theta \quad (37)$$

where  $\beta$  is the ratio of the inner radius of the annular plate to the outer radius.

The clamped boundary conditions at the outer edge of the plate ( $\rho = 1$ ) are:

$$W = 0 \quad (38)$$

$$\frac{\partial W}{\partial \rho} = 0 \quad (39)$$

$$U = 0 \quad (40)$$

$$V = 0 \quad (41)$$

#### IV. SOLUTION TO THE PROBLEM

The terms on the right hand side of the two von Karman equations (eqs. 13 and 20) represent the coupling effect between the lateral displacement and the in-plane stresses, and they are small compared to the left hand side of the equations for the range of displacements considered here. In fact, neglecting the right hand sides entirely, leads to the governing equations of linear, small-deflection plate theory. Thus the von Karman equations are suitable for solution by a systematic iteration procedure. If the lateral displacement and stress function are known to some degree of approximation, they can be used to evaluate the coupling effects in order to obtain the governing equations for the next higher approximation. The linear, small-deflection solution, obtained by neglecting the coupling effects, is the first approximation from which higher approximations are developed.

By using the lateral displacement obtained from linear theory, new expressions for the stress function and lateral displacement are obtained. These new expressions are called the second approximation and they can be used to develop a third approximation, and the third approximation used to develop a fourth approximation and so on. However, in the iteration procedure, the algebra inherently becomes more involved with higher approximations and only the second approximation



is obtained here. Higher approximations are discussed in more detail in Section C of this chapter.

A. First Approximation.

The governing equation for the first approximation to the lateral displacement is obtained by neglecting the right hand side of equation (20). The resulting equation ( $\nabla^4 W = 0$ ) is the governing equation of small-deflection theory and the solution as presented by H. Reissner (13) is:

$$W_1 = \alpha (A\rho + B\rho^3 + C\rho^{-1} + F\rho \ln \rho) \cos \theta \quad (42)$$

where A, B, C and F are constants of integration\*. The boundary conditions used to determine A, B, C and F are found from equations (34), (35), (38) and (39) by keeping only the terms linear in  $\alpha$ . The following expressions are obtained for the constants:

$$\begin{aligned} B &= \frac{-1}{2(1-\beta^2 + (1+\beta^2) \ln \beta)} \\ A &= (\beta^2 - 1) B \\ C &= -\beta^2 B \\ F &= -2(1+\beta^2) B \end{aligned} \quad (43)$$

---

\* Subscripts on displacements and resultants indicate the order of  $\alpha$  involved (i.e.: 1 indicates linear in  $\alpha$ , 2 indicates  $\alpha^2$  etc.)

Using the moment-curvature relationships (eqs. 17, 18, 19) and equation (42), the following expressions for the moment and shear resultants are obtained:

$$\begin{aligned}
 M_{r1} &= -\alpha (S_2 + \nu S_1) \cos \theta \\
 M_{\theta 1} &= -\alpha (S_1 + \nu S_2) \cos \theta \\
 M_{r\theta 1} &= -\alpha(1 - \nu) S_1 \sin \theta \\
 Q_{r1} &= -2\alpha(4B - F\rho^{-2}) \cos \theta \\
 Q_{\theta 1} &= 2\alpha(4B + F\rho^{-2}) \sin \theta
 \end{aligned} \tag{44}$$

where:

$$\begin{aligned}
 S_1 &= 2B\rho - 2C\rho^{-3} + F\rho^{-1} \\
 S_2 &= 6B\rho + 2C\rho^{-3} + F\rho^{-1}
 \end{aligned} \tag{45}$$

The expression for the moment applied to the rigid inclusion in order to cause the inclusion to rotate through an angle  $\alpha$ , is found by considering the equilibrium of moments acting on a free-body diagram of the entire plate. Summation of moments about the y axis gives:

$$\begin{aligned}
 -m - \int_0^{2\pi} (q_r a d\theta) a \cos \theta + \int_0^{2\pi} (m_r a d\theta) \cos \theta \\
 + \int_0^{2\pi} (m_{r\theta} a d\theta) \sin \theta = 0
 \end{aligned} \tag{46}$$

where the quantities  $q_r$ ,  $m_r$ , and  $m_{r\theta}$  are evaluated at the outer boundary ( $\rho = 1$ ). After integration and substitution of dimensionless variables, equation (46) becomes:

$$M_1 = -4\pi F\alpha \quad (47)$$

where  $F$  is defined in equations (43). From equation (47) it is seen the dimensionless applied moment for small deflections is independent of the inner and outer radius of the plate and depends only on their ratio ( $\beta$ ).

#### B. Second Approximation (First Iteration).

The linear, small-deflection solution for the lateral displacement (eq. 42) is used as an initial approximation to obtain a second approximation to the lateral displacement and in-plane stresses for nonlinear, large-deflections. The right hand side of the first von Karman equation (eq. 13) represents the stretching of the middle surface of the plate caused by lateral displacement, and for the second approximation this effect is determined from the lateral displacement given by linear theory. By substituting the expression for  $W_1$  from equation (42) into the right hand side of equation (13), the following governing equation for the second approximation to the stress function is obtained:

$$\nabla^4 \varphi = -12(1-\nu^2) \lambda^2 \alpha^2 \left[ 4 B^2 \rho^2 + 2 BF + 2 CF \rho^{-4} - 4 C^2 \rho^{-6} + \cos 2\theta (8 B^2 \rho^2 + 6 BF + (F^2 - 8 BC) \rho^{-2} - 2 CF \rho^{-4}) \right] \quad (48)$$

where B, C, and F are constants in the small deflection solution.

Being guided by the boundary conditions (eqs. 36 and 37), the solution to the homogeneous part of equation (48) is taken as:

$$\varphi_H = -12(1-\nu^2) \lambda^2 \alpha^2 \left[ B_0 \rho^2 + C_0 \ln \rho + D_0 \rho^2 \ln \rho + \cos 2\theta (A_2 \rho^2 + B_2 \rho^{-2} + C_2 \rho^4 + D_2) \right] \quad (49)$$

and upon adding a particular solution, the expression for the stress function becomes:

$$\varphi_2 = -12(1-\nu^2) \lambda^2 \alpha^2 \left[ B_0 \rho^2 + C_0 \ln \rho + D_0 \rho^2 \ln \rho + \frac{B^2}{144} \rho^6 + \frac{BF}{32} \rho^4 - \frac{C^2}{16} \rho^{-2} + \frac{CF}{4} \ln^2 \rho + \cos 2\theta \left[ A_2 \rho^2 + B_2 \rho^{-2} + C_2 \rho^4 + D_2 + \frac{B^2}{48} \rho^6 + \ln \rho \left( \frac{BF}{8} \rho^4 - \frac{(F^2 - 8BC)}{16} \rho^2 - \frac{CF}{8} \right) \right] \right] \quad (50)$$

Since the boundary conditions are prescribed on the in-plane displacements, expressions for U and V as functions of the stress function are found by combining equations (6), (7) and (8) with equations (9), (10) and (11). The resulting expressions are:

$$\frac{\partial U}{\partial \rho} + \frac{1}{2} \left( \frac{\partial W}{\partial \rho} \right)^2 = \frac{\lambda^{-2}}{12(1-\nu^2)} \left[ \frac{1}{\rho} \frac{\partial \varphi}{\partial \rho} + \frac{1}{\rho^2} \frac{\partial^2 \varphi}{\partial \theta^2} - \nu \frac{\partial^2 \varphi}{\partial \rho^2} \right] \quad (51)$$

$$\frac{U}{\rho} + \frac{1}{\rho} \frac{\partial V}{\partial \theta} + \frac{1}{2} \left( \frac{1}{\rho} \frac{\partial W}{\partial \theta} \right)^2 = \frac{\lambda^{-2}}{12(1-\nu^2)} \left[ \frac{\partial^2 \varphi}{\partial \rho^2} - \nu \left( \frac{1}{\rho} \frac{\partial \varphi}{\partial \rho} + \frac{1}{\rho^2} \frac{\partial^2 \varphi}{\partial \theta^2} \right) \right] \quad (52)$$

$$\frac{1}{\rho} \frac{\partial U}{\partial \theta} - \frac{V}{\rho} + \frac{\partial V}{\partial \rho} + \frac{1}{\rho} \frac{\partial W}{\partial \rho} \frac{\partial W}{\partial \theta} = \frac{-\lambda^2}{6(1-\nu)} \frac{\partial}{\partial \rho} \left( \frac{1}{\rho} \frac{\partial \varphi}{\partial \theta} \right) \quad (53)$$

Integrating equations (51) and (52) once, U and V can be written as:

$$U = \frac{\lambda^{-2}}{12(1-\nu^2)} \int \left[ \frac{1}{\rho} \frac{\partial \varphi}{\partial \rho} + \frac{1}{\rho^2} \frac{\partial^2 \varphi}{\partial \theta^2} - \nu \frac{\partial^2 \varphi}{\partial \rho^2} \right] d\rho - \frac{1}{2} \int \left( \frac{\partial W}{\partial \rho} \right)^2 d\rho + h(\theta) \quad (54)$$

$$V = \frac{\rho \lambda^{-2}}{12(1-\nu^2)} \int \left[ \frac{\partial^2 \varphi}{\partial \rho^2} - \nu \left( \frac{1}{\rho} \frac{\partial \varphi}{\partial \rho} + \frac{1}{\rho^2} \frac{\partial^2 \varphi}{\partial \theta^2} \right) \right] d\theta - \int U d\theta - \frac{\rho}{2} \int \left( \frac{1}{\rho} \frac{\partial W}{\partial \theta} \right)^2 d\theta + g(\rho) \quad (55)$$

where for the second approximation  $\varphi$  is given by equation (50),  $W_1$  by equation (42) and  $h(\theta)$  and  $g(\rho)$  are arbitrary functions of integration.

To obtain expressions for  $h(\theta)$  and  $g(\rho)$ , equations (54) and (55) are substituted into the remaining strain-displacement equation (eq. 53) and the following equation is obtained:

$$\frac{1}{\rho} \frac{dh}{d\theta} - \frac{1}{\rho} \left[ g - \int h d\theta \right] + \frac{dg}{d\rho} = 0 \quad (56)$$

Ordinary differential equations for  $h(\theta)$  and  $g(\rho)$  are obtained by separating variables in equation (56), and the solutions of the differential equations give the following displacements resulting from  $h(\theta)$  and  $g(\rho)$ :

$$U = L_1 \cos \theta + L_2 \sin \theta \quad (57)$$

$$V = L_2 \cos \theta - L_1 \sin \theta + L_3 \rho \quad (58)$$

where  $L_1$ ,  $L_2$  and  $L_3$  are constants. Non-zero values of  $L_1$  and  $L_2$  correspond to rigid body displacements and non-zero values of  $L_3$  correspond to a rigid body rotation of the plate. Therefore these constants must be equal to zero for the plate considered in this investigation, and consequently  $h(\theta)$  and  $g(\rho)$  also vanish.

Performing the integrations in equations (54) and (55), the following expressions for the in-plane displacements are obtained.

$$U = -\alpha^2 \left[ \gamma_1(\rho) + \gamma_2(\rho) \cos 2\theta \right] \quad (59)$$

$$V = \alpha^2 \left[ \rho\theta \left( \frac{F^2}{4} - 2 BC - 4 D_0 \right) + \gamma_3(\rho) \sin 2\theta \right] \quad (60)$$

The displacements arising from the first term in equation (60) are different for  $(\theta)$  and  $(\theta+2\pi)$  and therefore the constant  $D_0$  must be selected so as to cause this multi-valued term to vanish. Hence, the constant  $D_0$  is given by:

$$16 D_0 = F^2 - 8 BC \quad (61)$$

$\gamma_1(\rho)$ ,  $\gamma_2(\rho)$  and  $\gamma_3(\rho)$  are functions of the radial coordinate, which contain the six undetermined constants ( $B_0$ ,  $C_0$ ,  $A_2$ ,  $B_2$ ,  $C_2$ ,  $D_2$ ), and are given by:

$$\begin{aligned}
 \gamma_1(\rho) = \frac{1}{4} & \left\{ \frac{B^2}{6} (11-\nu)\rho^5 + \left[ 2 AB + \frac{BF}{2} (3-\nu) \right] \rho^3 + 8 [B_0(1-\nu) \right. \\
 & + \frac{3-\nu}{4} F^2 - 2 BC (2-\nu) + A^2] \rho + \left[ 2C(A+F) - 4(1+\nu)C_0 \right] \rho^{-1} \\
 & - \frac{C^2}{2} (1+\nu)\rho^{-3} + \ln \rho \left[ 2 BF \rho^3 + \left[ 2 AF + \frac{(1-\nu)}{2} (F^2 - 8 BC) \right] \rho \right. \\
 & \left. \left. - 2 CF \nu \rho^{-1} + F^2 \rho \ln \rho \right] \right\} \quad (62)
 \end{aligned}$$

$$\begin{aligned}
 \gamma_2(\rho) = \frac{1}{4} & \left\{ \frac{B^2}{6} (11-3\nu) \rho^5 + \left[ 2 AB + \frac{BF}{2} (3-\nu) - 16 \nu C_2 \right] \rho^3 \right. \\
 & + \left[ A^2 + \frac{F^2}{4} (1+\nu) - 2 \nu BC - 8(1+\nu)A_2 \right] \rho + \left[ \frac{CF}{2} (5+\nu) \right. \\
 & + 2 AC + 16 D_2 \left. \right] \rho^{-1} + \left[ 8 B_2(1+\nu) - \frac{C^2}{3} \right] \rho^{-3} \\
 & + \ln \rho \left[ 2 BF (1-\nu)\rho^3 + \left( 2 AF + \frac{(1+\nu)}{2} (F^2 - 8 BC) \right) \rho \right. \\
 & \left. \left. + F^2 \rho \ln \rho \right] \right\} \quad (63)
 \end{aligned}$$

$$\begin{aligned}
 \gamma_3(\rho) = \frac{1}{8} & \left\{ \frac{B^2}{3} (1-\nu)\rho^5 + \left[ 4 AB - 2 BF - 16(3+\nu) C_2 \right] \rho^3 \right. \\
 & + \left[ 2 A^2 + F^2 - 4 BC - 16 A_2(1+\nu) \right] \rho + \left[ 2 CF + 4 AC \right. \\
 & + 16 D_2(1-\nu) \left. \right] \rho^{-1} + \left[ \frac{2C^2}{3} - 16 B_2(1+\nu) \right] \rho^{-3} \\
 & + \ln \rho \left[ - 2 BF(1+\nu)\rho^3 + \left( 4 AF + (1+\nu)(F^2 - 8 BC) \right) \rho \right. \\
 & \left. \left. + 2 CF(1+\nu) \rho^{-1} + 2 F^2 \rho \ln \rho \right] \right\} \quad (64)
 \end{aligned}$$

Applying the boundary conditions on the in-plane displacements (eqs. 36, 37, 40 and 41), where only terms of order  $\alpha^2$  are retained, the following expressions for the six constants in the stress function equation (eq. 50) are obtained:

$$\begin{aligned}
 B_0 &= \frac{\beta^2}{8(1-\nu)(1-\beta^2)} [R_1 - \beta^{-2} R_2] \\
 C_0 &= \frac{\beta^2}{4(1+\nu)(1-\beta^2)} [R_1 - R_2] \\
 C_2 &= \frac{\left\{ \beta^2(1+\nu) [2(R_3 - R_4) + (1-\beta^4)(R_4 - R_6)] \right. \\
 &\quad \left. - [3-\nu + (1+\nu)\beta^2][R_3 - R_5 - \beta^4(R_4 - R_6)] \right\}}{\left\{ \beta^2(1-\beta^2)[2(3+\nu) + (3-\nu)\beta^2(1+\beta^2)] \right. \\
 &\quad \left. + \left(\frac{3-\nu}{1+\nu}\right)(1-\beta^6)[3-\nu + (1+\nu)\beta^2] \right\}} \\
 D_2 &= \frac{R_3 - R_5 - \beta^4(R_4 - R_6) - C_2 \left(\frac{3-\nu}{1+\nu}\right)(1-\beta^6)}{1-\beta^2} \\
 B_2 &= \frac{1}{2} \left[ R_3 - R_5 - D_2 - \left(\frac{3-\nu}{1+\nu}\right)C_2 \right] \\
 A_2 &= R_3 - B_2 - \left(\frac{3+\nu}{1+\nu}\right)C_2 + \left(\frac{1-\nu}{1+\nu}\right)D_2
 \end{aligned} \tag{65}$$



where:

$$R_1 = \frac{B^2}{6}(11-\nu)\beta^4 + \left[ 2AB + \frac{BF}{2}(3-\nu) \right] \beta^2 + \left[ A^2 + \left(\frac{3-\nu}{4}\right)F^2 - 2BC(2-\nu) - 1 \right] \\ + 2C(A+F)\beta^{-2} - \frac{C^2}{2}(1+\nu)\beta^{-4} + \ln \beta \left[ 2BF\beta^2 + 2AF + \left(\frac{1-\nu}{2}\right)(F^2 - 8BC) \right. \\ \left. - 2CF\nu\beta^{-2} + F^2 \ln \beta \right]$$

$$R_2 = \frac{B^2}{6}(11-\nu) - \frac{C^2}{2}(1+\nu) + 2AB + BF\left(\frac{3-\nu}{2}\right) + 2AC + 2CF + \left(\frac{3-\nu}{4}\right)F^2 \\ - 2BC(2-\nu) + A^2$$

$$R_3 = \frac{1}{16(1+\nu)} \left\{ \frac{B^2}{3}(1-\nu) - 2BF + 4AB + 2CF + 4AC + 2A^2 + F^2 \right. \\ \left. - 4BC + \frac{2C^2}{3} \right\}$$

$$R_4 = \frac{1}{16(1+\nu)} \left\{ \frac{B^2}{3}(1-\nu)\beta^4 + 2B(2A-F)\beta^2 + (2A^2 + F^2 - 4BC - 2) + 2C(2A+F)\beta^{-2} \right. \\ \left. + \frac{2C^2}{3}\beta^{-4} + \ln \beta \left[ -2BF(1+\nu)\beta^2 + (F^2 - 8BC)(1+\nu) + 4AF \right. \right. \\ \left. \left. + 2CF(1+\nu)\beta^{-2} + 2F^2 \ln \beta \right] \right\}$$

$$R_5 = \frac{1}{16(1+\nu)} \left\{ \frac{B^2}{3}(11-3\nu) + 4AB + BF(3-\nu) + 2A^2 + F^2\left(\frac{1+\nu}{2}\right) - 4\nu BC \right. \\ \left. + CF(5+\nu) + 4AC - \frac{2}{3}C^2 \right\}$$

$$R_6 = \frac{1}{16(1+\nu)} \left\{ \frac{B^2}{3}(11-3\nu)\beta^4 + \left[ 4AB + BF(3-\nu) \right] \beta^2 + \left[ 2A^2 + F^2\left(\frac{1+\nu}{2}\right) \right. \right. \\ \left. \left. - 4\nu BC - 2 \right] + \left[ 4AC + CF(5+\nu) \right] \beta^{-2} - \frac{2C^2}{3}\beta^{-4} + \ln \beta \left[ 4BF(1-\nu)\beta^2 \right. \right. \\ \left. \left. + 4AF + (F^2 - 8BC)(1+\nu) + 2F^2 \ln \beta \right] \right\} \quad (66)$$

Equation (50) is differentiated to obtain the following expressions for the in-plane stress resultants:

$$\begin{aligned}
 N_r &= -12(1-\nu^2)\lambda^2 [S_3 + S_4 \cos 2\theta] \alpha^2 \\
 N_\theta &= -12(1-\nu^2)\lambda^2 [S_5 + S_6 \cos 2\theta] \alpha^2 \\
 N_{r\theta} &= 24(1-\nu^2)\lambda^2 [S_7 \sin 2\theta] \alpha^2
 \end{aligned} \tag{67}$$

where:

$$\begin{aligned}
 S_3 &= \frac{B^2}{24} \rho^4 + \frac{BF}{8} \rho^2 + 2B_0 + D_0 + C_0 \rho^{-2} + \frac{C^2}{8} \rho^{-4} + \ln \rho \left[ 2D_0 + \frac{CF}{2} \rho^{-2} \right] \\
 S_4 &= \frac{B^2}{24} \rho^4 + \frac{BF}{8} \rho^2 - 2A_2 - \left( \frac{F^2 - 8BC}{16} \right) - \left( 4D_2 + \frac{CF}{8} \right) \rho^{-2} - 6B_2 \rho^{-4} \\
 &\quad + \ln \rho \left[ \frac{F^2 - 8BC}{8} + \frac{CF}{2} \rho^{-2} \right] \\
 S_5 &= \frac{5}{24} B^2 \rho^4 + \frac{3BF}{8} \rho^2 + 2B_0 + 3D_0 + \left( \frac{CF}{2} - C_0 \right) \rho^{-2} - \frac{3}{8} C^2 \rho^{-4} \\
 &\quad + \ln \rho \left[ 2D_0 - \frac{CF}{2} \rho^{-2} \right] \\
 S_6 &= \frac{5}{8} B^2 \rho^4 + \left( \frac{7BF}{8} + 12C_2 \right) \rho^2 + 2A_2 - \frac{3}{16} (F^2 - 8BC) + \frac{CF}{8} \rho^{-2} \\
 &\quad + 6B_2 \rho^{-4} + \ln \rho \left[ \frac{3BF}{2} \rho^2 - \frac{(F^2 - 8BC)}{8} \right] \\
 S_7 &= \frac{5}{48} B^2 \rho^4 + \left( \frac{BF}{8} + 3C_2 \right) \rho^2 + A_2 - \left( \frac{F^2 - 8BC}{16} \right) - \left( \frac{CF}{8} + D_2 \right) \rho^{-2} \\
 &\quad - 3B_2 \rho^{-4} + \ln \rho \left[ \frac{3BF}{8} \rho^2 - \left( \frac{F^2 - 8BC}{16} \right) + \frac{CF}{8} \rho^{-2} \right]
 \end{aligned} \tag{68}$$

The right hand side of the second von Karman equation (eq. 20), which represents the reduction in lateral displacement due to the in-plane forces, can now be evaluated by using the first approximation for lateral displacement (eq. 42) and the expression for the stress function (eq. 50). The following linear governing equation for the second approximation of lateral displacement is obtained:

$$\nabla^4 W = -12(1-\nu^2)\lambda^2 \left[ \gamma_6(\rho) \cos \theta + \gamma_7(\rho) \cos 3\theta \right] \alpha^3 \quad (69)$$

where:

$$\begin{aligned} \gamma_6(\rho) = & B^3 \rho^5 + \frac{21}{8} B^2 F \rho^3 + (16BB_0 + 12BD_0 + \frac{B^2 C}{2} - 8BA_2 + \frac{5BF^2}{8}) \rho \\ & + (4BC_0 - 8BD_2 + 4F(B_0 + D_0) - 2FA_2 + \frac{BCF}{2}) \rho^{-1} + (\frac{5}{8} CF^2 \\ & + BC^2 - 4CD_0) \rho^{-3} + (4CC_0 - 8CD_2 + 6FB_2 - 2C^2 F) \rho^{-5} \\ & + C(C^2 - 24B_2) \rho^{-7} + \ln \rho \left[ (16BD_0 + \frac{B}{2} (F^2 - 8BC)) \rho + (2BCF \right. \\ & \left. + 4FD_0 + \frac{F^3}{8}) \rho^{-1} + 3C^2 F \rho^{-5} \right] \\ \gamma_7(\rho) = & \frac{7}{6} B^3 \rho^5 + (24BC_2 + \frac{55}{24} B^2 F) \rho^3 + (12FC_2 + \frac{BF^2}{8} + 4B^2 C) \rho \\ & + (2FA_2 - 16BD_2 - \frac{F^3}{4} - 24CC_2) \rho^{-1} + (\frac{CF^2}{8} - 24BB_2 - 8CA_2 \\ & - 3BC^2 - 4FD_2) \rho^{-3} + (\frac{C^2 F}{4} - 6FB_2) \rho^{-5} + \ln \rho \left[ 3B^2 F \rho^3 \right. \\ & \left. + \frac{3}{2} BF^2 \rho - \frac{F^3}{8} \rho^{-1} + (CF^2 - 4BC^2) \rho^{-3} \right] \end{aligned} \quad (70)$$

The homogeneous solution to equation (69) is:

$$\begin{aligned} W_H = W_1 - 12(1-\nu^2)\lambda^2 \alpha^3 \left[ (A_1 \rho + B_1 \rho^3 + C_1 \rho^{-1} + D_1 \rho \ln \rho) \cos \theta \right. \\ \left. + (A_3 \rho^3 + B_3 \rho^{-3} + C_3 \rho^5 + D_3 \rho^{-1}) \cos 3\theta \right] \end{aligned} \quad (71)$$

where  $W_1$  is the linear solution (eq.42) and  $A_1, B_1, C_1, D_1, A_3, B_3, C_3$  and  $D_3$  are eight constants to be determined from boundary conditions. A particular solution to equation (69) is added to the homogeneous solution and the expression for the lateral displacement to order  $\alpha^3$  becomes:

$$\begin{aligned}
 W = W_1 - 12(1-\nu^2)\lambda^2\alpha^3 & \left[ (A_1\rho + B_1\rho^3 + C_1\rho^{-1} + D_1\rho \ln\rho + R_{10}\rho^9 \right. \\
 & + R_{11}\rho^7 + R_{12}\rho^5 + R_{13}\rho^5 \ln\rho + R_{14}\rho^3 \ln\rho + R_{15}\rho^3 \ln^2\rho \\
 & + R_{16}\rho \ln^2\rho + R_{17}\rho^{-1} \ln\rho + R_{18}\rho^{-1} \ln^2\rho + R_{19}\rho^{-3}) \cos\theta \\
 & + (A_3\rho^3 + B_3\rho^{-3} + C_3\rho^5 + D_3\rho^{-1} + R_{20}\rho^9 + R_{21}\rho^7 + R_{22}\rho^7 \ln\rho \\
 & + R_{23}\rho^5 \ln\rho + R_{24}\rho^5 \ln^2\rho + R_{25}\rho^3 \ln\rho + R_{26}\rho^3 \ln^2\rho + R_{27}\rho \\
 & \left. + R_{28}\rho \ln\rho + R_{29}\rho^{-1} \ln\rho) \cos 3\theta \right] \quad (72)
 \end{aligned}$$

where:

$$R_{10} = B^3/3840$$

$$R_{11} = [7/3072] B^2 F$$

$$R_{12} = \frac{BB_0}{12} - \frac{5}{144} BD_0 + \frac{1}{4608} BF^2 + \frac{31}{1152} B^2 C - \frac{BA_2}{24}$$

$$R_{13} = \frac{BD_0}{12} + \frac{BF^2}{384} - \frac{B^2 C}{48}$$

$$R_{14} = \frac{BC_0}{4} - \frac{BD_2}{2} - \frac{FD_0}{16} + \frac{FB_0}{4} - \frac{FA_2}{8} - \frac{BCF}{8} - \frac{5}{512} F^3$$

$$R_{15} = \frac{BCF}{16} + \frac{FD_0}{8} + \frac{F^3}{256}$$

$$R_{16} = \frac{CD_0}{2} - \frac{5}{64} CF^2 - \frac{BC^2}{8}$$

$$R_{17} = \frac{CD_2}{2} - \frac{CC_0}{4} - \frac{3FB_2}{8} - \frac{7}{64} C^2 F$$

$$R_{18} = -\frac{3}{32} C^2 F$$

$$\begin{aligned}
 R_{19} &= \frac{C}{192} (C^2 - 24B_2) \\
 R_{20} &= \frac{7}{17,280} B^3 \\
 R_{21} &= \frac{3}{80} BC_2 - \frac{19}{19,200} B^2F \\
 R_{22} &= \frac{3}{640} B^2F \\
 R_{23} &= -\frac{17}{1536} BF^2 + \frac{FC_2}{8} + \frac{B^2C}{24} \\
 R_{24} &= \frac{BF^2}{128} \\
 R_{25} &= \frac{BD_2}{3} + \frac{CC_2}{2} - \frac{FA_2}{24} + \frac{25}{4608} F^3 \\
 R_{26} &= \frac{F^3}{768} \\
 R_{27} &= \frac{1}{64} \left[ \frac{CF^2}{8} - 24BB_2 - 8CA_2 - 3BC^2 - 4FD_2 \right] \\
 R_{28} &= \frac{C}{64} \left[ F^2 - 4BC \right] \\
 R_{29} &= \frac{F}{48} \left[ \frac{C^2}{4} - 6B_2 \right]
 \end{aligned} \tag{73}$$

Applying the boundary conditions on W as given in equations (34), (35), (38) and (39), the following expressions for the eight constants in equation (72) are obtained:

$$\begin{aligned}
 c_1 &= \left\{ \beta^2(1-\beta^2) \left[ (1-\beta^2)(R_{33}-R_{31}) - 2(R_{31}-R_{32}) \right] \right. \\
 &\quad \left. - \beta^2(1-\beta^2 + 2 \ln \beta) \left[ R_{34} - R_{32} - \beta^2 (R_{33} - R_{31}) \right] \right\} \\
 &\quad \frac{1}{2(1-\beta^2) \left[ (1+\beta^2)(1-\beta^2 + 2 \ln \beta) + (1-\beta^2)^2 \right]} \\
 D_1 &= \frac{1}{1-\beta^2} \left[ R_{34}-R_{32}-\beta^2(R_{33}-R_{31}) + 2\beta^{-2}(1-\beta^4)c_1 \right]
 \end{aligned}$$

$$B_1 = \frac{1}{2} \left[ R_{33} - R_{31} + 2C_1 - D_1 \right]$$

$$A_1 = R_{31} - B_1 - C_1$$

(74)

where:

$$R_{31} = -(R_{10} + R_{11} + R_{12} + R_{19})$$

$$R_{32} = \frac{\lambda^{-2}}{72(1-\nu^2)} - \left\{ R_{10}\beta^8 + R_{11}\beta^6 + R_{12}\beta^4 + R_{19}\beta^{-4} + \ln\beta \left[ R_{13}\beta^4 + R_{14}\beta^2 + R_{17}\beta^{-2} \right] + \ln^2\beta \left[ R_{15}\beta^2 + R_{16} + R_{18}\beta^{-2} \right] \right\}$$

$$R_{33} = -(9R_{10} + 7R_{11} + 5R_{12} + R_{13} + R_{14} + R_{17} - 3R_{19})$$

$$R_{34} = \frac{\lambda^{-2}}{72(1-\nu^2)} - \left\{ 9R_{10}\beta^8 + 7R_{11}\beta^6 + (3R_{12} + R_{13})\beta^4 + R_{14}\beta^2 + R_{17}\beta^{-2} - 3R_{19}\beta^{-4} + \ln\beta \left[ 5R_{13}\beta^4 + (3R_{14} + 2R_{15})\beta^2 + 2R_{16} + (2R_{18} - R_{17})\beta^{-2} \right] + \ln^2\beta \left[ 3R_{15}\beta^2 + R_{16} - R_{18}\beta^{-2} \right] \right\}$$

(75)

and

$$D_3 = \frac{3\beta^4}{2} \left\{ (1-\beta^8) \left[ R_{36}(1+\beta^6) - 2R_{35} + (1-\beta^6)R_{38} \right] + (4\beta^2 - \beta^8 - 3) \left[ R_{35} - R_{37} - \beta^6(R_{36}-R_{38}) \right] \right\} \\ \frac{\hspace{10em}}{(1-\beta^8)(1+2\beta^6-3\beta^4) + 2\beta^4(1-\beta^2)(4\beta^2-\beta^8-3)}$$

$$C_3 = \frac{3 \left[ R_{35} - R_{37} - \beta^6(R_{36}-R_{38}) \right] - 4(1-\beta^2) D_3}{2(\beta^8-1)}$$

$$B_3 = \frac{R_{35} - R_{37}}{2} + \frac{C_3 - 2D_3}{3}$$

$$A_3 = R_{35} - B_3 - C_3 - D_3$$

(76)

where:

$$\begin{aligned}
 R_{35} &= - \left[ R_{20} + R_{21} + R_{27} \right] \\
 R_{36} &= - \left\{ R_{20}\beta^6 + R_{21}\beta^4 + R_{27}\beta^{-2} + \ln\beta \left[ R_{22}\beta^4 + R_{23}\beta^2 + R_{25} + R_{28}\beta^{-2} \right. \right. \\
 &\quad \left. \left. + R_{29}\beta^{-4} \right] + \ln^2\beta \left[ R_{24}\beta^2 + R_{26} \right] \right\} \\
 R_{37} &= - \frac{1}{3} \left[ 9R_{20} + 7R_{21} + R_{22} + R_{23} + R_{25} + R_{27} + R_{28} + R_{29} \right] \\
 R_{38} &= - \frac{1}{3} \left\{ 9R_{20}\beta^6 + (7R_{21} + R_{22})\beta^4 + R_{23}\beta^2 + R_{25} + (R_{27} + R_{28})\beta^{-2} \right. \\
 &\quad \left. + R_{29}\beta^{-4} + \ln\beta \left[ 7R_{22}\beta^4 + (5R_{23} + 2R_{24})\beta^2 + (3R_{25} + 2R_{26}) \right. \right. \\
 &\quad \left. \left. + R_{28}\beta^{-2} - R_{29}\beta^{-4} \right] + \ln^2\beta \left[ 5R_{24}\beta^2 + 3R_{26} \right] \right\} \tag{77}
 \end{aligned}$$

Equation (72) yields the following expressions for shear and

moment resultants:

$$\begin{aligned}
 M_r &= M_{r1} + M_{r3} \\
 M_\theta &= M_{\theta1} + M_{\theta3} \\
 M_{r\theta} &= M_{r\theta1} + M_{r\theta3} \\
 Q_r &= Q_{r1} + Q_{r3} \\
 Q_\theta &= Q_{\theta1} + Q_{\theta3} \tag{78}
 \end{aligned}$$

where  $M_{r1}$ ,  $M_{\theta1}$ ,  $M_{r\theta1}$ ,  $Q_{r1}$  and  $Q_{\theta1}$  are given by equations (44) and the terms of order  $\alpha^3$  by:

$$\begin{aligned}
 M_{r3} &= 12(1-\nu^2)\lambda^2\alpha^3 \left[ (S_8 + \nu S_9)\cos\theta + (S_{10} + \nu S_{11})\cos 3\theta \right] \\
 M_{\theta3} &= 12(1-\nu^2)\lambda^2\alpha^3 \left[ (S_9 + \nu S_8)\cos\theta + (S_{11} + \nu S_{10})\cos 3\theta \right]
 \end{aligned}$$

$$\begin{aligned}
 M_{r03} &= 12(1-\nu^2)(1-\nu)\lambda^2\alpha^3 \left[ S_9 \sin\theta + 3 S_{12} \sin 3\theta \right] \\
 Q_{r3} &= 12(1-\nu^2)\lambda^2\alpha^3 \left[ S_{13} \cos\theta + S_{14} \cos 3\theta \right] \\
 Q_{\theta 3} &= -12(1-\nu^2)\lambda^2\rho^{-1}\alpha^3 \left[ (S_8 + S_9) \sin\theta + 3(S_{10} + S_{11}) \sin 3\theta \right] \quad (79)
 \end{aligned}$$

where:

$$\begin{aligned}
 S_8 &= 72 R_{10}\rho^7 + 42 R_{11}\rho^5 + (20R_{12} + 9R_{13})\rho^3 + (5R_{14} + 2R_{15} \\
 &\quad + 6B_1)\rho + (2R_{16} + D_1)\rho^{-1} + (-3R_{17} + 2R_{18} + 2C_1)\rho^{-3} \\
 &\quad + 12 R_{19}\rho^{-5} + \ln\rho \left[ 20R_{13}\rho^3 + (6R_{14} + 10R_{15})\rho + 2 R_{16}\rho^{-1} \right. \\
 &\quad \left. + (2R_{17} - 6R_{18})\rho^{-3} \right] + \ln^2\rho \left[ 2R_{15}\rho + 2R_{18}\rho^{-3} \right]
 \end{aligned}$$

$$\begin{aligned}
 S_9 &= 8 R_{10}\rho^7 + 6 R_{11}\rho^5 + (4R_{12} + R_{13})\rho^3 + (R_{14} + 2B_1)\rho + D_1\rho^{-1} \\
 &\quad + (R_{17} - 2C_1)\rho^{-3} - 4 R_{19}\rho^{-5} + \ln\rho \left[ 4R_{13}\rho^3 + 2(R_{14} + R_{15})\rho \right. \\
 &\quad \left. + 2 R_{16}\rho^{-1} + 2(R_{18} - R_{17})\rho^{-3} \right] + \ln^2\rho \left[ 2R_{15}\rho - 2R_{18}\rho^{-3} \right]
 \end{aligned}$$

$$\begin{aligned}
 S_{10} &= 72 R_{20}\rho^7 + (42R_{21} + 13R_{22})\rho^5 + (9R_{23} + 2R_{24} + 20C_3)\rho^3 \\
 &\quad + (5R_{25} + 2R_{26} + 6A_3)\rho + R_{28}\rho^{-1} + (-3R_{29} + 2D_3)\rho^{-3} + 12B_3\rho^{-5} \\
 &\quad + \ln\rho \left[ 42R_{22}\rho^5 + (20R_{23} + 18R_{24})\rho^3 + (6R_{25} + 10R_{26})\rho \right. \\
 &\quad \left. + 2R_{29}\rho^{-3} \right] + \ln^2\rho \left[ 20R_{24}\rho^3 + 6R_{26}\rho \right]
 \end{aligned}$$

$$\begin{aligned}
 S_{11} &= (R_{22} - 2R_{21})\rho^5 + (R_{23} - 4C_3)\rho^3 + (R_{25} - 6A_3)\rho + (R_{28} - 8R_{27})\rho^{-1} \\
 &\quad + (R_{29} - 10D_3)\rho^{-3} - 12B_3\rho^{-5} + \ln\rho \left[ -2R_{22}\rho^5 + (2R_{24} - 4R_{23})\rho^3 \right. \\
 &\quad \left. + (2R_{26} - 6R_{25})\rho - 8R_{28}\rho^{-1} - 10R_{29}\rho^{-3} \right] + \ln^2\rho \left[ -4R_{24}\rho^3 - 6R_{26}\rho \right]
 \end{aligned}$$



$$\begin{aligned}
 S_{12} &= 8 R_{20} \rho^7 + (6R_{21} + R_{22}) \rho^5 + (R_{23} + 4C_3) \rho^3 + (R_{25} + 2A_3) \rho \\
 &+ R_{28} \rho^{-1} + (R_{29} - 2D_3) \rho^{-3} - 4B_3 \rho^{-5} + \ln \rho \left[ 6R_{22} \rho^5 \right. \\
 &+ (4R_{23} + 2R_{24}) \rho^3 + 2(R_{25} + R_{26}) \rho - 2R_{29} \rho^{-3} \left. \right] \\
 &+ \ln^2 \rho \left[ 4R_{24} \rho^3 + 2R_{26} \rho \right] \\
 S_{13} &= 540 R_{10} \rho^6 + 240 R_{11} \rho^4 + (72R_{12} + 54R_{13}) \rho^2 + 14(R_{14} + R_{15}) \\
 &+ 8 B_1 + 2(R_{16} - D_1) \rho^{-2} + (6R_{17} - 10R_{18}) \rho^{-4} - 40 R_{19} \rho^{-6} \\
 &+ \ln \rho \left[ 72R_{13} \rho^2 + 8R_{14} + 28R_{15} - 4R_{16} \rho^{-2} + 12R_{18} \rho^{-4} \right] \\
 &+ \ln^2 \rho \left[ 4R_{15} \right] \\
 S_{14} &= 504 R_{20} \rho^6 + (200 R_{21} + 110 R_{22}) \rho^4 + (46 R_{23} + 26 R_{24} + \\
 &+ 48 C_3) \rho^2 + 6 R_{25} + 14 R_{26} + (8 R_{27} - 10 R_{28}) \rho^{-2} \\
 &+ (32 D_3 - 2 R_{29}) \rho^{-4} + \ln \rho \left[ 200 R_{22} \rho^4 + (48 R_{23} + 92 R_{24}) \rho^2 \right. \\
 &+ 12 R_{26} + 8 R_{28} \rho^{-2} + 36 R_{29} \rho^{-4} \left. \right] + 48 R_{24} \rho^2 \ln^2 \rho \quad (80)
 \end{aligned}$$

The maximum bending and membrane stresses are found from the usual flexural and axial load formulas, where dimensionless stresses have been formed by dividing the actual stress by the modulus of elasticity.  $\sigma'$  and  $\sigma''$  are used to denote the dimensionless membrane and bending stresses respectively, and these are given by:

$$\sigma_r' = \frac{N_r}{12(1-\nu^2)\lambda^2} \quad \sigma_\theta' = \frac{N_\theta}{12(1-\nu^2)\lambda^2} \quad (81)$$

$$\sigma_r'' = \frac{M_{r1} + M_{r3}}{2(1-\nu^2)\lambda} \quad \sigma_\theta'' = \frac{M_{\theta1} + M_{\theta3}}{2(1-\nu^2)\lambda} \quad (82)$$

and the dimensionless bending stresses from linear theory by:

$$\sigma_{r1}'' = \frac{M_{r1}}{2(1-\nu^2)\lambda} \quad \sigma_{\theta1}'' = \frac{M_{\theta1}}{2(1-\nu^2)\lambda} \quad (83)$$

The applied moment found from equations (46), (47) and (79) is:

$$M = M_1 + M_3 \quad (84)$$

where  $M_1$  is given by equation (47) and  $M_3$  by:

$$M_3 = -12(1-\nu^2)\lambda^2 \pi \alpha^3 \left[ 480 R_{10} + 192 R_{11} + 48 R_{12} + 44 R_{13} + 8 R_{14} + 12 R_{15} + 8 R_{17} - 12 R_{18} - 48 R_{19} - 4D_1 \right] \quad (85)$$

$M_3$  represents the additional moment required to overcome the added stiffness introduced by the membrane forces in order to obtain the same angle of rotation as predicted by linear theory. Equation (85) shows that the second approximation yields an applied moment which depends on the radius-thickness ratio ( $\lambda$ ) as well as the ratio of radii ( $\beta$ ), whereas the applied moment in linear theory depends only

upon  $\beta$ . It should be recalled the moment referred to here is the dimensionless moment, whereas the actual physical moment is the plate stiffness multiplied by the dimensionless moment.

### C. Discussion.

Since the development of this investigation is based on a perturbation from the linear solution, the small angle of rotation ( $\alpha$ ) is used to determine the order of magnitude of various terms. The first approximation (linear theory) leads to bending stresses and lateral displacement which are  $O(\alpha)$ . Thus derivatives of  $W$  are  $O(\alpha)$  and products of its derivatives are  $O(\alpha^2)$ .

The second approximation gives in-plane displacements and stresses of  $O(\alpha^2)$  and a reduction in lateral displacement of  $O(\alpha^3)$ . Derivatives of  $U$  and  $V$  are of  $O(\alpha^2)$  and their products of  $O(\alpha^4)$ . Thus, the terms neglected in the strain-displacement relations (eqs. 9, 10, and 11) are of  $O(\alpha^4)$  and are small compared to the nonlinear terms of  $O(\alpha^2)$  retained. However, if another iteration were performed to obtain a third approximation, the right hand side of the first von Karman equation (eq. 13) would involve terms of  $O(\alpha^4)$ . Therefore it would seem inconsistent to obtain a third approximation involving terms of the same order as those neglected by the governing equation.

However, as can be seen from equations (59), (60) and (72), the nonlinear terms of  $O(\alpha^4)$  involving the lateral displacement contain

a multiplying factor of  $\lambda^2$  which is not present in the nonlinear terms of  $O(\alpha^4)$  involving the in-plane displacements. Therefore for large  $\lambda$ , the nonlinear terms neglected in the von Karman equations are still small and the iteration can be continued without being inconsistent. This observation has also been confirmed by unpublished work (2) done by the author's thesis advisor in which it was found that for rotationally symmetric problems the extra terms in E. Reissner's more exact equations (see reference 10) contribute negligible corrections to the corresponding solutions obtained from the von Karman equations if the plate is thin.

At this point it seems worthwhile to include a brief qualitative discussion of the effect of thickness on large deflections. For a very thin plate (i.e., a membrane), the bending terms in the von Karman equations are negligible and the appropriate governing equations for the membrane can be obtained from the von Karman equations by letting the plate stiffness vanish ( $D \rightarrow 0$ ). For plates too thick to be called membranes, but yet thin enough so that the extra terms in Reissner's equations are small, the von Karman equations apply. The Reissner equations should be used for thicker plates. Of course, the magnitude of the loading also determines which set of equations are appropriate, and in fact determines whether a large deflection analysis is needed.

An interesting combination of the membrane and von Karman equations has been treated in the literature for axisymmetric bending of circular

plates. Even though the bending stiffness of a plate is not negligible, for fairly large deflections the plate behaves essentially as a membrane except in a small region near the boundary. In the region near the boundary, called the boundary layer, the bending becomes very important. This phenomenon can be observed in Figure 11, where the bending stresses are nearly zero in the central one-third of the annulus and much larger than the membrane stresses near the boundary.

Very recently, E. Reissner derived a more exact set of governing equations for unsymmetrical deformations, which are the counterpart of his equations for symmetric deformations. When these equations become available (see reference 12), perhaps the results of this investigation can be compared to his more exact theory.

Numerical results were obtained by programming the algebraic expressions developed in this chapter for the IBM 7040 digital computer. In all cases Poisson's ratio was assumed to be 0.33. Figure 3 shows the lateral displacement of points lying along the radial line normal to the axis of rotation (points along this line experience the maximum lateral and radial displacements), and it illustrates the reduction in lateral displacement caused by the in-plane stresses.

Figures 4 and 5 show the maximum in-plane displacements. By examining the slopes of these two curves and comparing them to the slope of the lateral displacement in Figure 3, for an angle of rotation of 1.5 degrees the magnitude of the nonlinear terms neglected in the

strain-displacement relations is found to be approximately one thousandth of the magnitude of those nonlinear terms retained.

Figures 6, 7, and 8 show the applied moment-angle of rotation relationships for various plate geometries. The ordinates of these curves represent the ratio of the dimensionless applied moment to that dimensionless moment from linear theory which would generate an angle of rotation equal to one degree for the particular plate considered. Thus one straight line represents the linear moment-rotation relationships for all plates. Figure 9 shows the same type of relationship for the radial bending stresses.

The variation of the stresses with applied moment is shown in Figure 10 and the variation of the stresses along the radial line normal to the axis of rotation is shown in Figure 11. The stresses shown in Figure 11 are for a dimensionless applied moment equal to 5.63, which corresponds to an angle of rotation of 1.5 degrees using the iteration solution or 4.95 degrees using linear theory. The effect of the thickness-radius ratio ( $\lambda$ ) on the maximum total radial stress is shown in Figure 12.

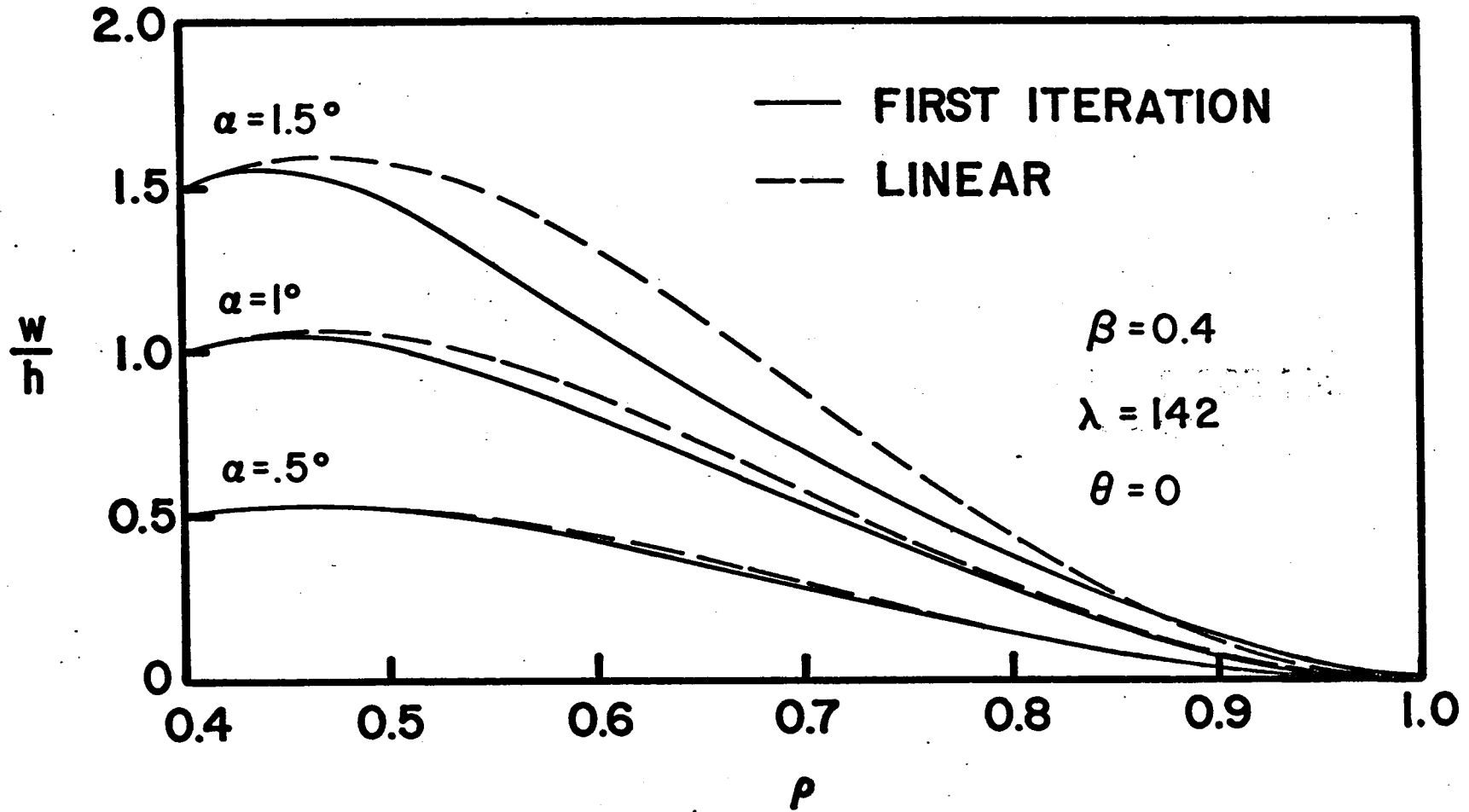


FIGURE 3. Lateral displacement along radial line normal to axis of rotation.

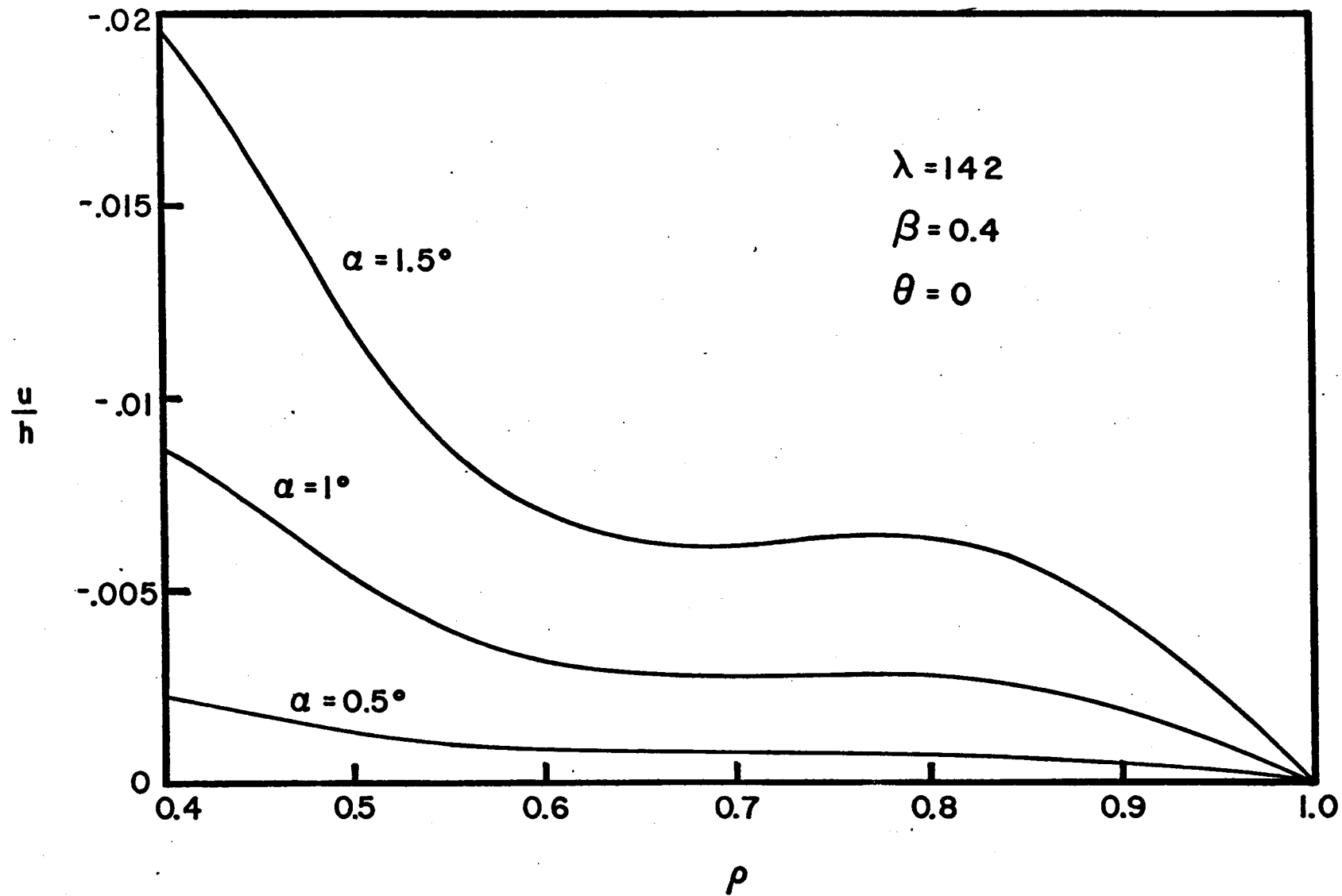


FIGURE 4. Radial displacement along radial line normal to axis of rotation



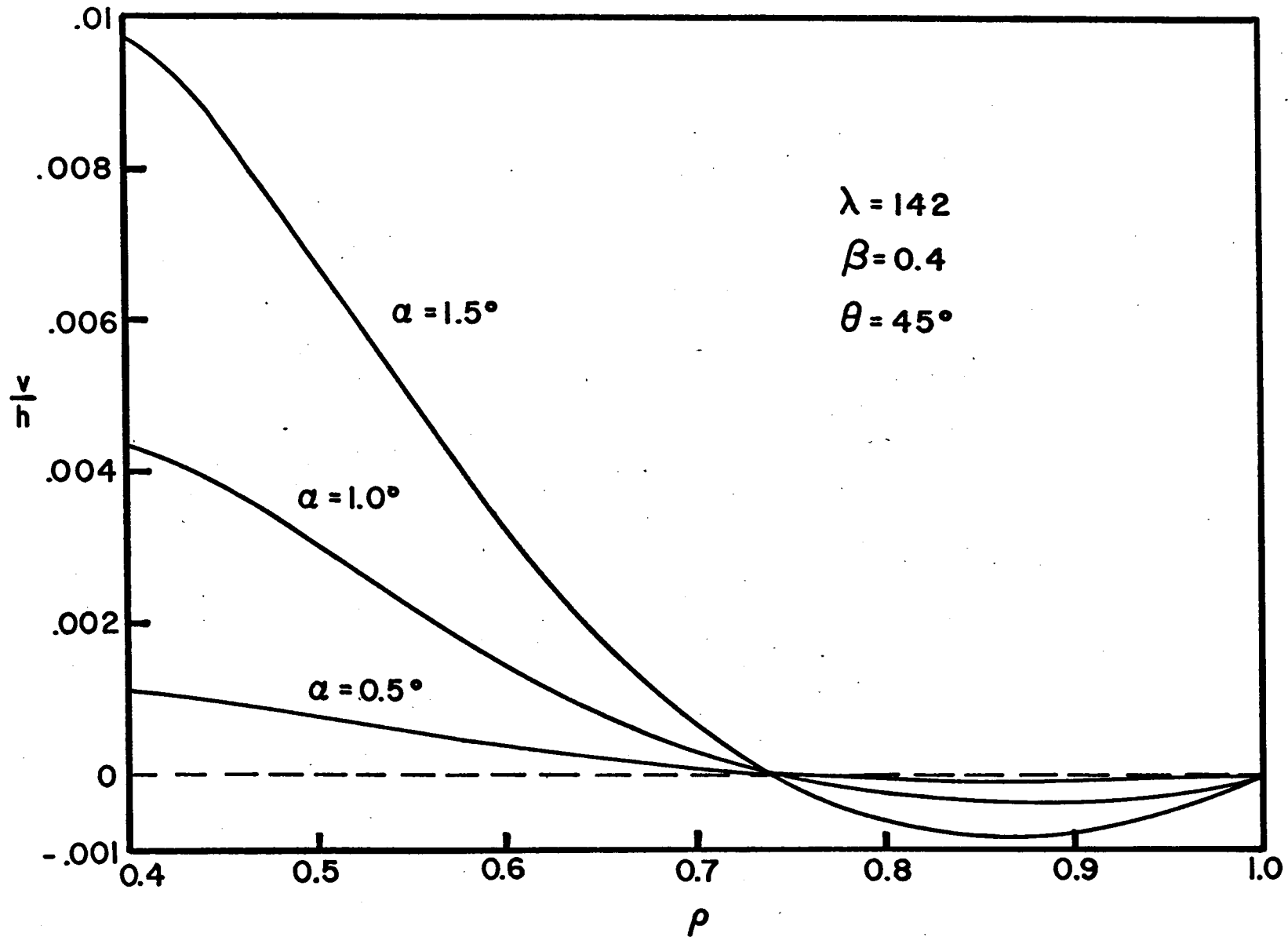


FIGURE 5. Maximum tangential displacement

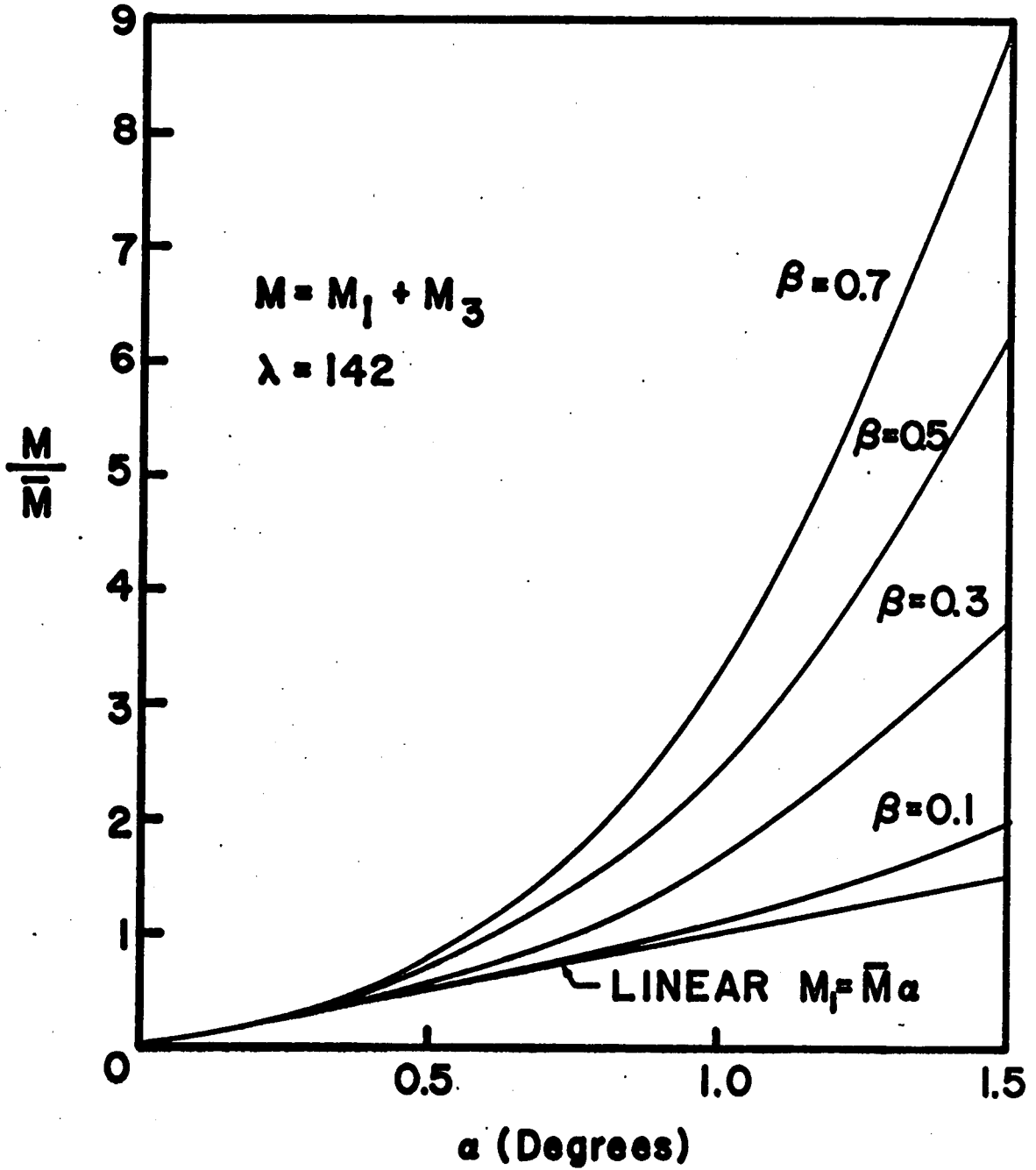


FIGURE 6. Applied moment-angle of rotation relationships

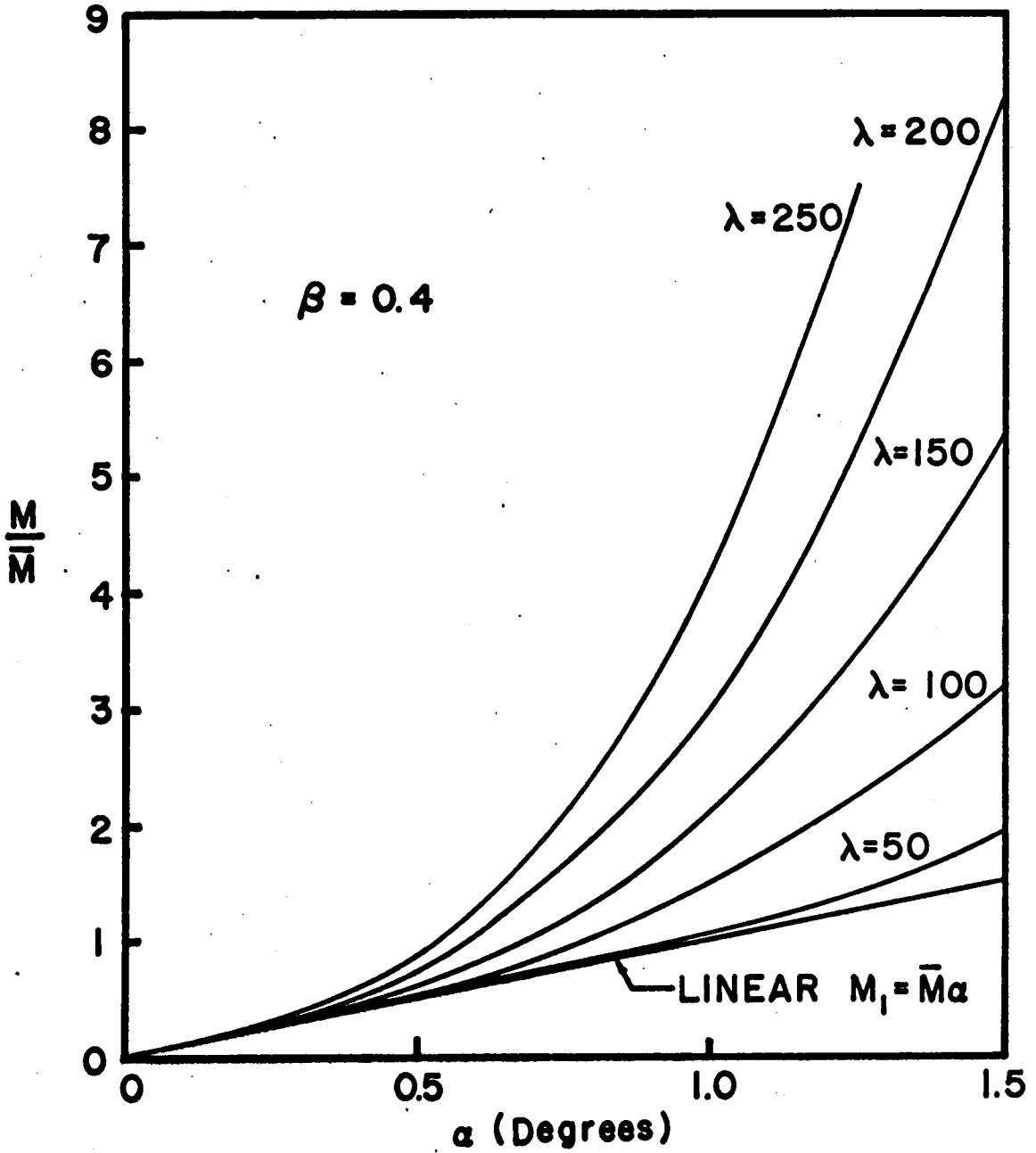


FIGURE 7. Effect of thickness on applied moment ( $\beta = 0.4$ )

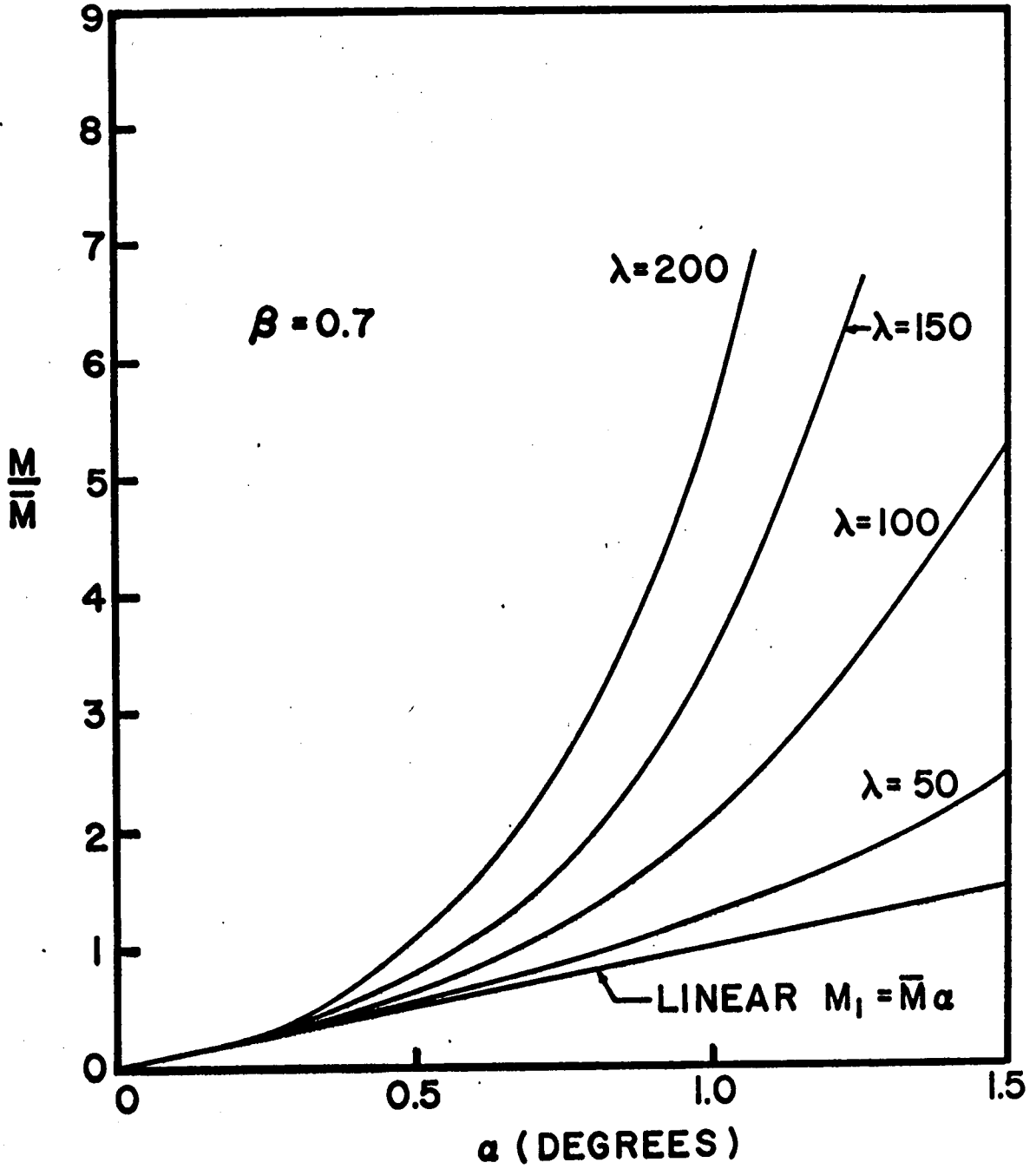


FIGURE 8. Effect of thickness on applied moment ( $\beta = 0.7$ )

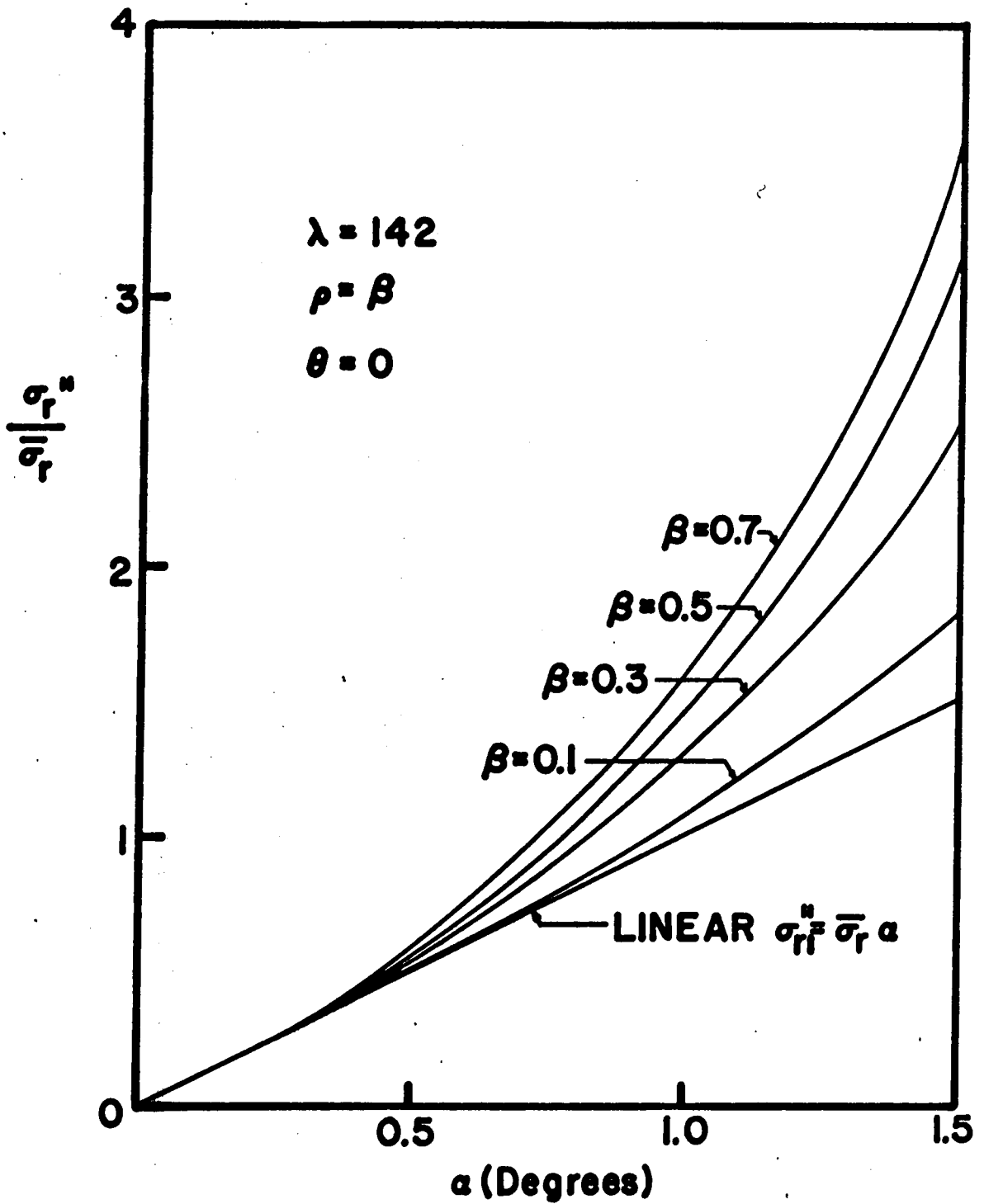


FIGURE 9. Maximum radial bending stress

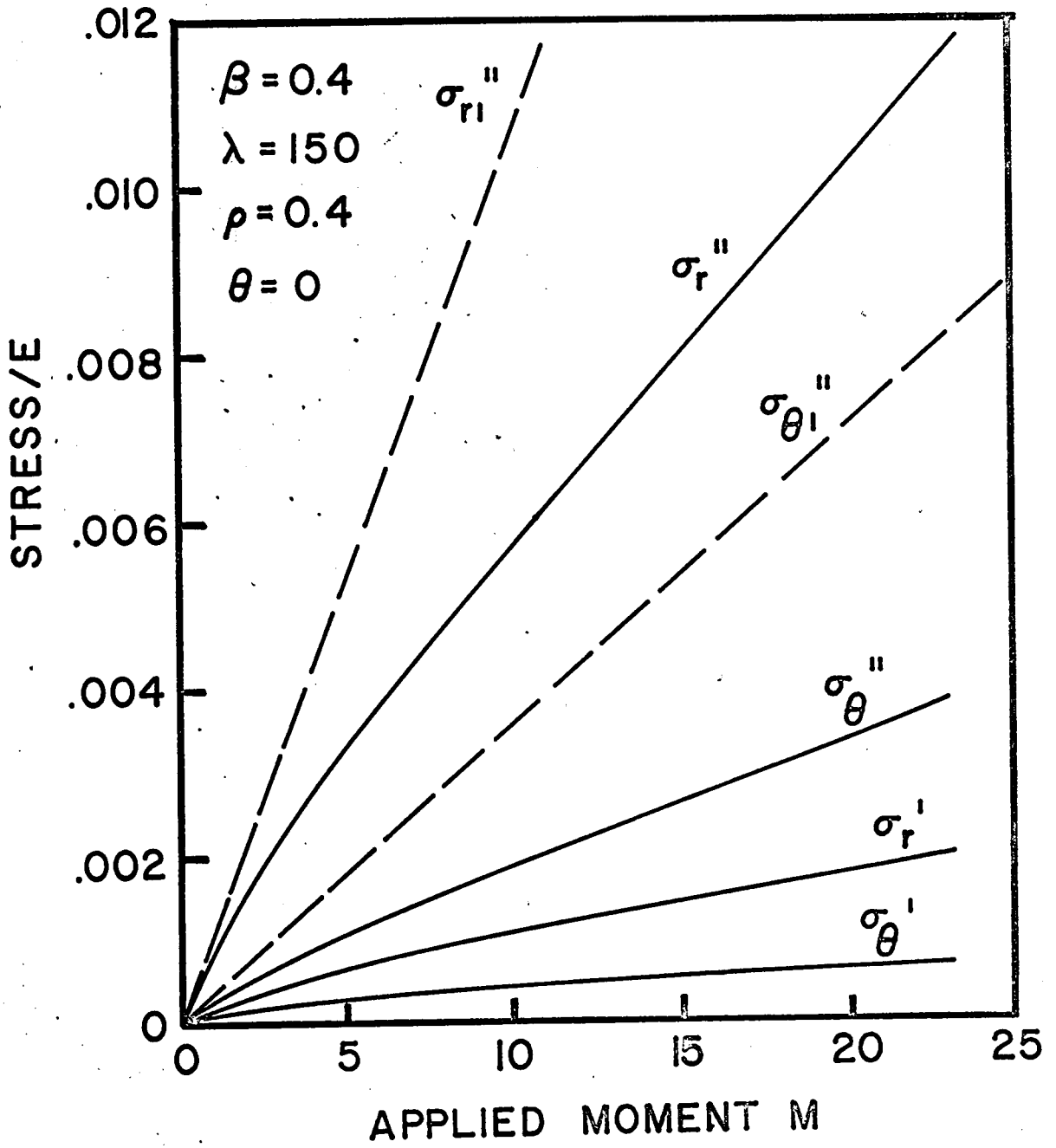


FIGURE 10. Maximum stresses

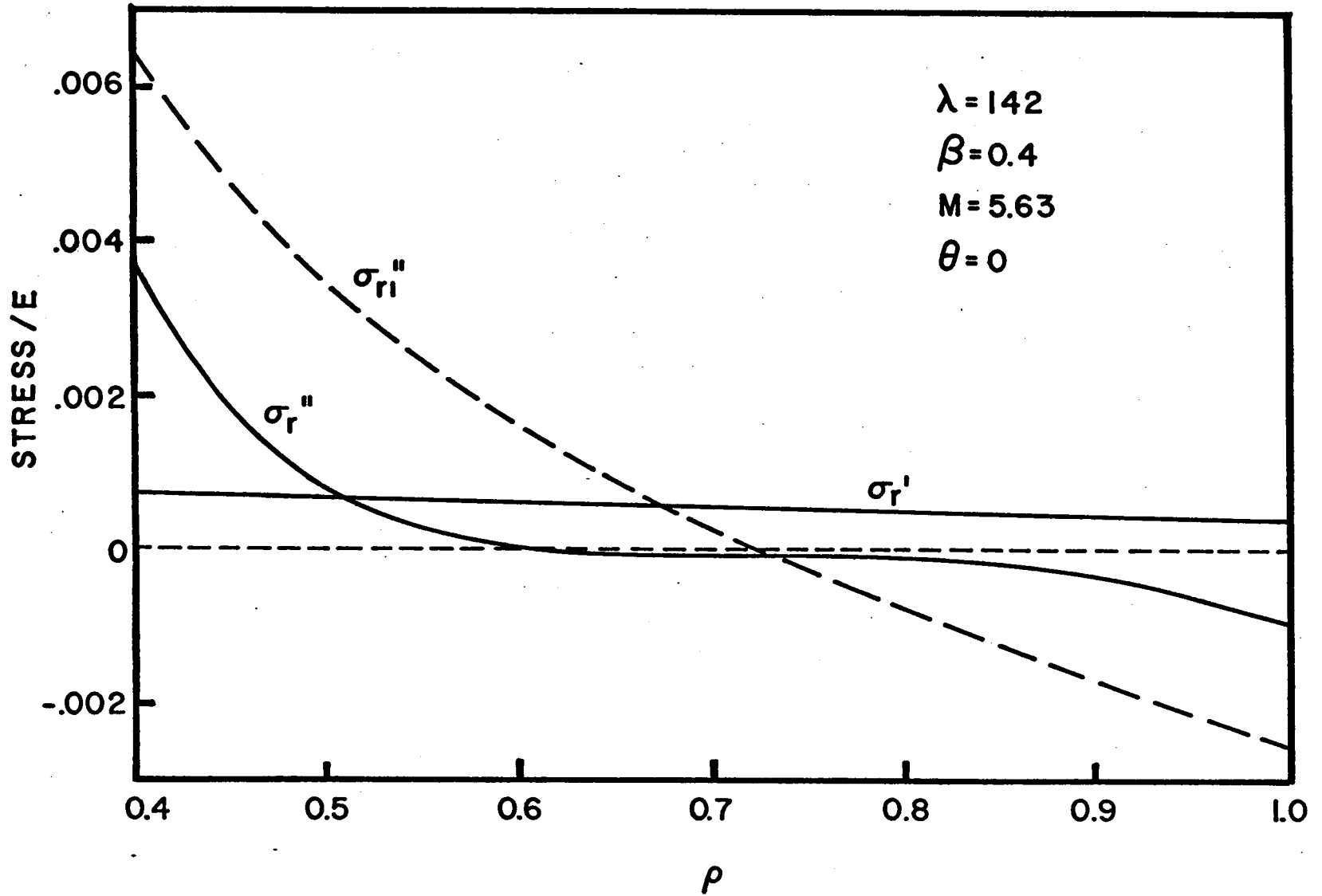


FIGURE 11. Variation of radial stresses along the line  $\theta = 0$ .

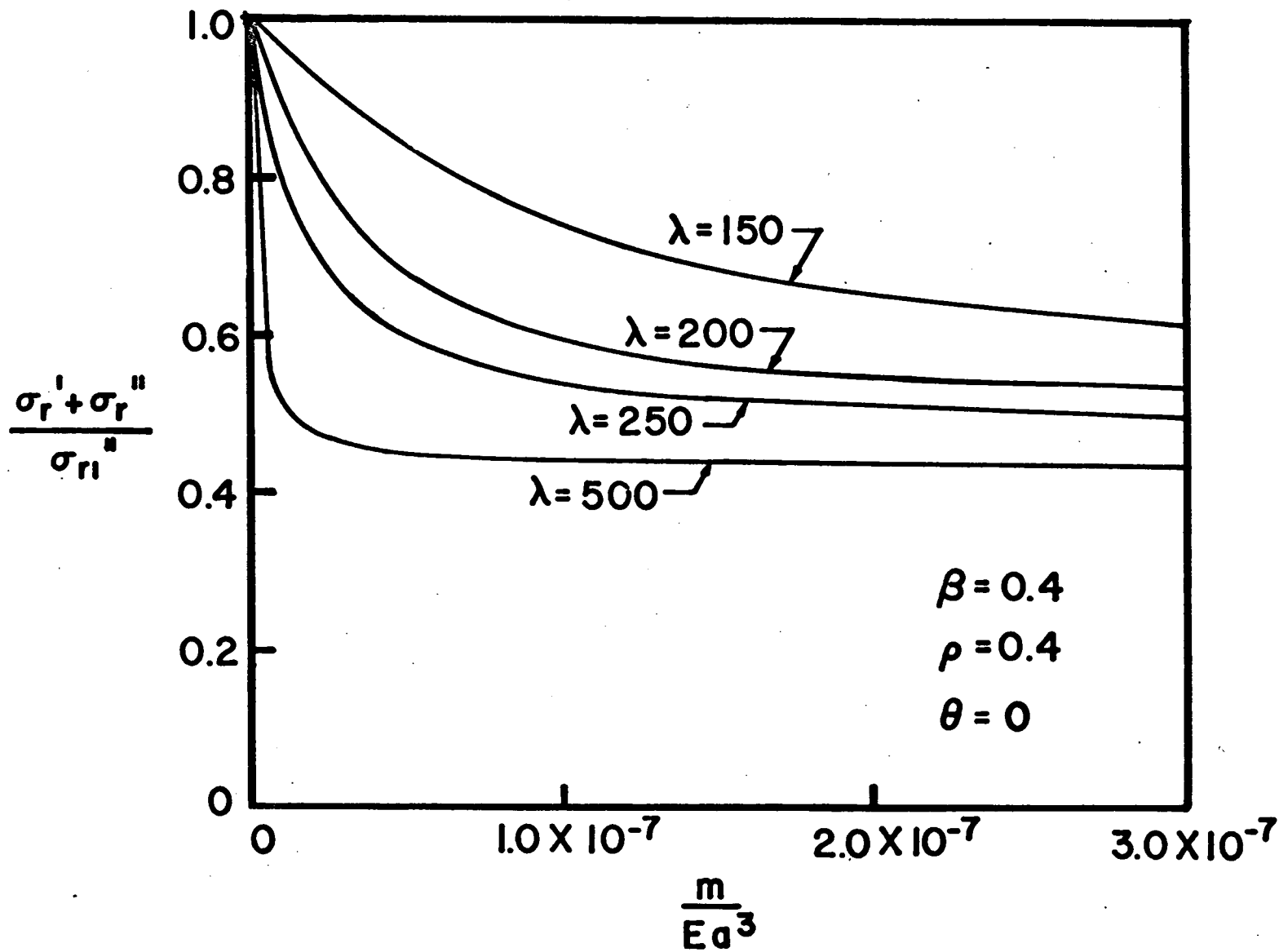


FIGURE 12. Maximum total radial stress ( $\beta = 0.4$ )



## V. EXPERIMENTAL INVESTIGATION

A brief description of the experimental apparatus used in this investigation is given in this chapter and the experimental results, which were obtained with the help of Liberty and Collier (8), are compared with the analytical solution presented in Chapter IV. Although Roark (14) had previously obtained experimental data for the same problem using a 24 inch diameter, 1/4 inch thick steel plate, his results are too limited to verify the analytical solutions developed in this investigation. Roark only reported the maximum stresses observed for one value of applied moment and did not give any indication of the magnitude of the displacements or rotations involved, although he did state in the report that only small deflections were to be considered.

### A. Experimental Apparatus.

Up to this point the problem has been pictured as the outer boundary of the annulus being stationary and the rigid inclusion rotated relative to it. However, it was felt the exact reverse situation in which the inclusion is stationary and the outer boundary rotated relative to the inclusion would be better for experimental purposes.

Experiments were conducted with an 18 inch outer diameter, 7.2 inch inner diameter plate made of 7075 - T6 aluminum. The plate

was 0.0634 inches thick and was found to have a modulus of elasticity of  $10 \times 10^6$  psi and a Poisson's ratio of 0.33. The annulus was formed by sandwiching a square piece of aluminum plate between two 1/4 inch thick steel plates in which central 18 inch diameter holes had been machined. The rigid inclusion was formed with machined 1/4 inch thick steel plates and was connected to a rigid support.

The outer boundary of the annulus was rotated relative to the central inclusion about a predetermined diameter of the annulus by applying weights so as to create a moment about the axis of rotation. In order to predetermine the axis of rotation and to keep the reactions of the apparatus and applied weights from being transferred to the inclusion, pivot bolts and supports were attached to the outer edge of the steel plates. Photographs of the experimental apparatus are shown in Figures 13 and 14.

Foil strain gages (1/4 in. x 1/8 in.) were mounted on the aluminum plate along the radial lines normal to the axis of rotation. The maximum strains occur at the inner boundary and are of most interest, but the radial strains at the outer boundary were also measured. In order to be able to separate the bending and membrane strains, gages were placed on both surfaces of the plate along one of the radial lines. Along the opposite radial line gages were placed only at points of maximum strain, and were used to provide a check on the symmetry of the strains. After some initial adjustments in the apparatus, a very high degree of symmetry was obtained.

Besides the radial strain, the applied moment and the resulting angle of rotation were measured. The angle of rotation was found by measuring the tangent of the angle with a rigid pointer.

B. Comparison Between Experiment and the Iteration Solution.

The experimental results obtained are given in Figures 15, 16 and 17, which show excellent agreement with the iteration solution for rotations up to 1.5 degrees (which corresponds to a lateral displacement at the inner boundary of about 1.5 times the thickness of the plate). For larger rotations the iteration solution begins to overestimate the nonlinear effect.

The applied moment-angle of rotation relationships are shown in Figure 15 and measured radial strain versus angle of rotation in Figures 16 and 17. Since gages could not be mounted right at the inner boundary, the strains shown in Figures 16 and 17 do not represent the absolute maximum strain in the plate. The measured radial coordinate of the centers of the innermost gages ( $\rho = 0.421$ ) is used to compute the theoretical radial strains from equations (81), (82), (83) and Hooke's law. For the particular plate tested, the iteration solution gives strains at the inner boundary ( $\rho = 0.4$ ) about 15 percent larger than those shown for  $\rho = 0.421$  in Figure 16.

The maximum radial strain shown in Figure 16 has been decomposed into the bending and membrane parts in Figure 17. It is interesting

to note that the experimental membrane strain is larger than that predicted by the iteration solution, which is in agreement with the statement made by Hart and Evans (6) that the von Karman equations underestimate the in-plane forces. Although there is better agreement between the bending strains from the iteration solution and the experiment up to 1.5 degrees of rotation, the experimental bending strains are slightly larger than the theoretical strains. One possible explanation of this is the effect of the thickness of the strain gages, which is not taken into account in the graph.

The agreement between the theoretical and experimental strains at the outer boundary is as good as that at the inner boundary.

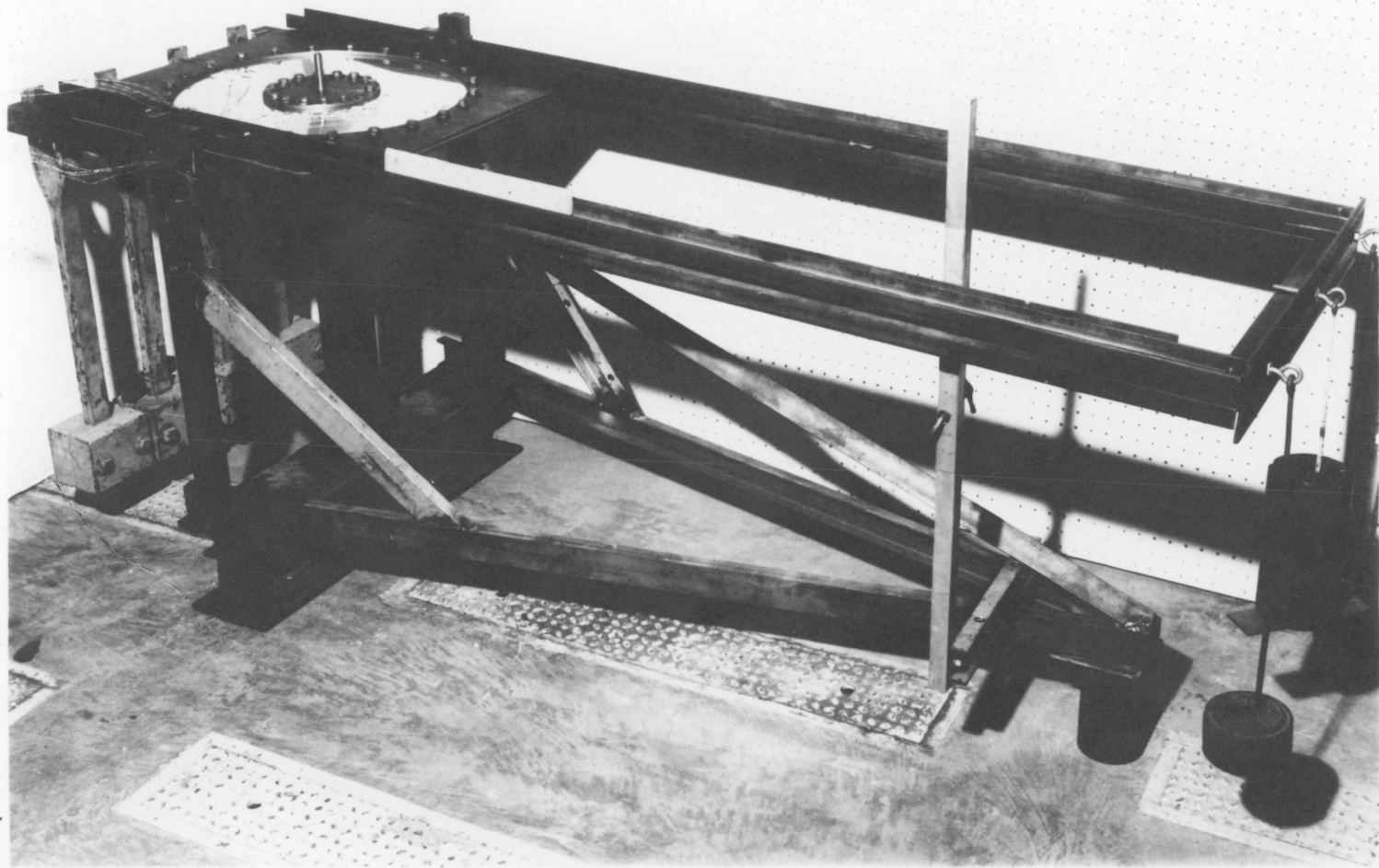


FIGURE 13. Experimental apparatus

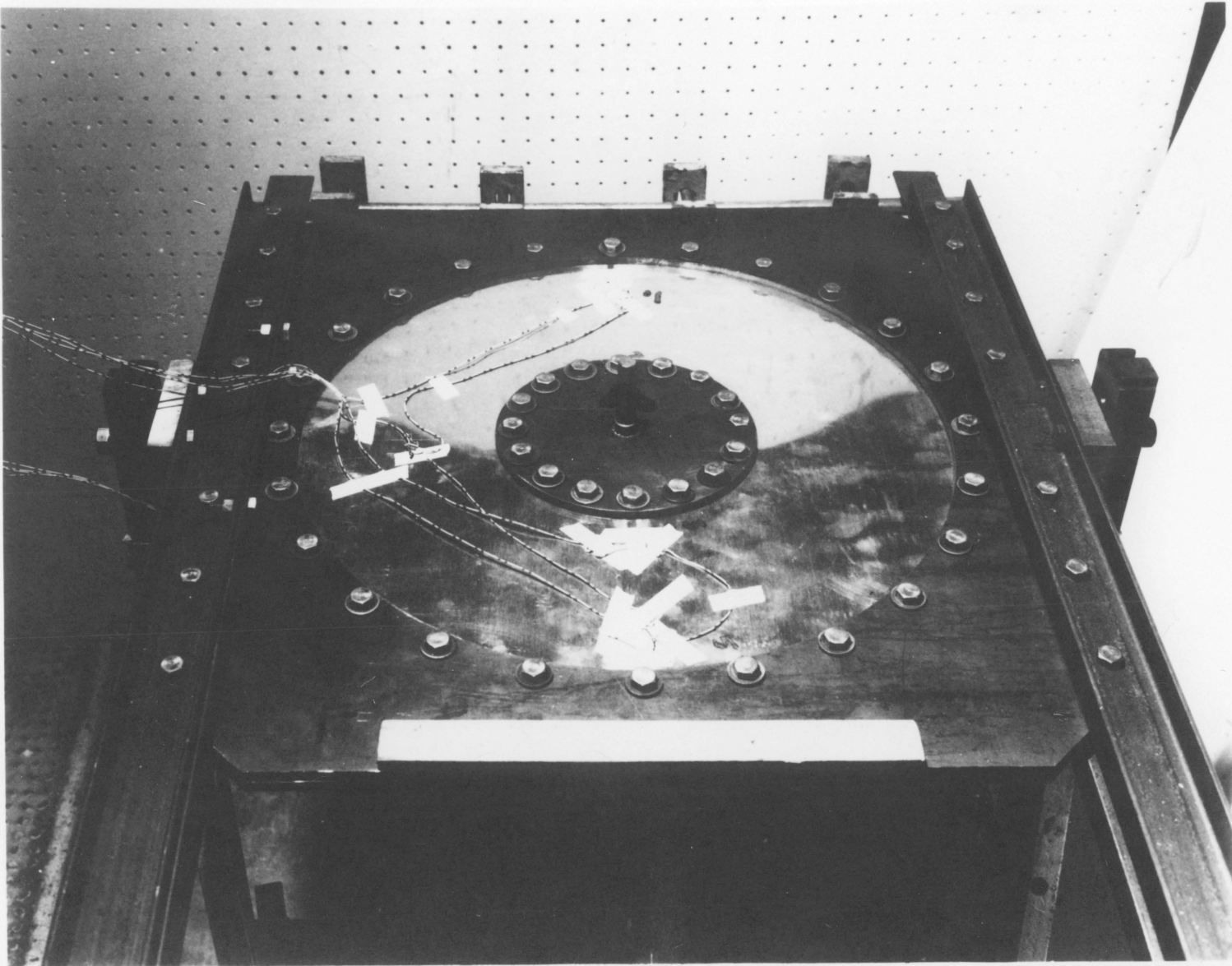


FIGURE 14. Experimental apparatus

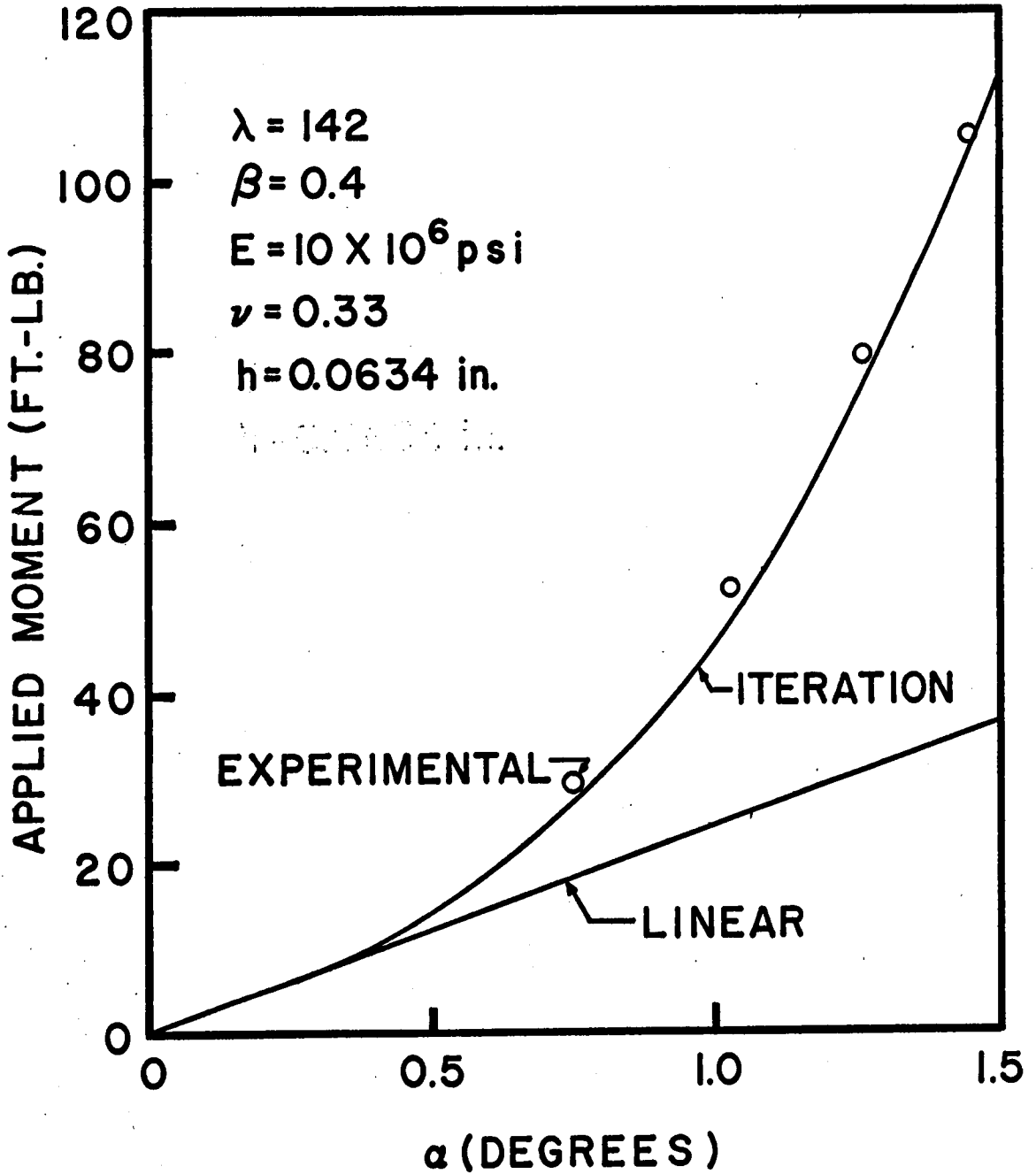


FIGURE 15. Experimental moment-rotation curve

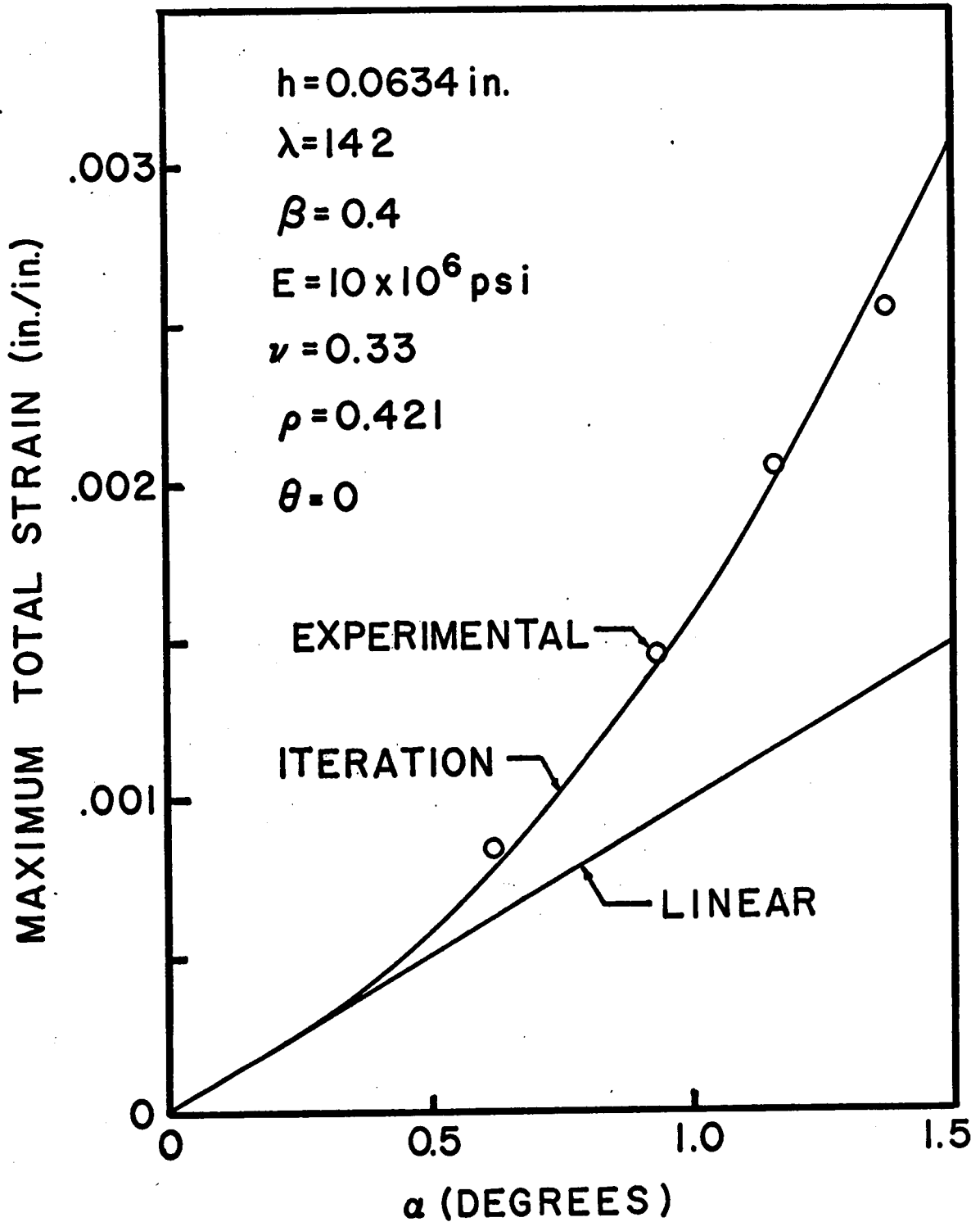


FIGURE 16. Experimental maximum total radial strain



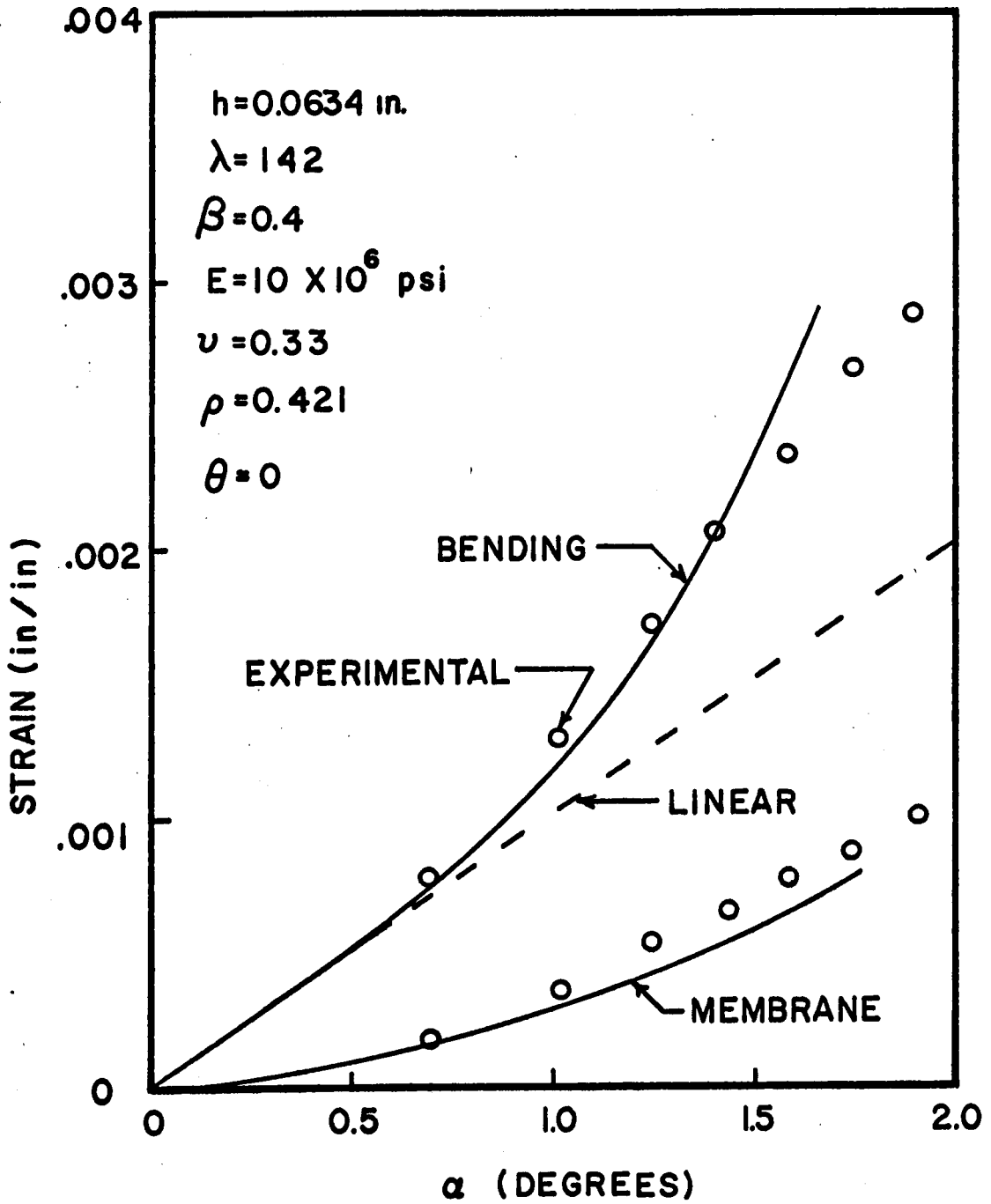


FIGURE 17. Experimental bending and membrane radial strains

## VI. CONCENTRATED MOMENT

If the radius of the rigid inclusion vanishes, an interesting limiting case of this investigation develops. With  $\beta = 0$ , the problem becomes a clamped circular plate with a concentrated moment about the y axis applied at the center of the plate. The solution for the concentrated moment is developed in this chapter by taking the limit as  $\beta$  approaches zero in the solution given in Chapter IV. Of course the solution can also be obtained by writing the boundary conditions for a circular plate (including the requirement that the displacements be finite at the center of the plate) and by following the same iteration scheme as was used in Chapter IV.

### A. Solution by Iteration.

As  $\beta$  approaches zero, the constants in the linear solution for the lateral displacement as given in equations (43) behave as follows:

$$\begin{aligned} B &\sim \frac{-1}{2 \ln \beta} \\ A &\sim -B \\ C &\sim -\beta^2 B \\ F &\sim -2B \end{aligned} \tag{86}$$

and from equation (47) the moment applied at the center of the plate is:

$$M = 8\pi B \alpha \tag{87}$$

Substituting equations (86) and (87) into the expression for the linear lateral displacement (eq. 42), the following equation is obtained:

$$W_1 = \frac{M}{8\pi} (-\rho + \rho^3 - \beta^2 \rho^{-1} - 2\rho \ln \rho) \cos \theta \quad (88)$$

In order to distinguish the quantities for the case of a concentrated moment from those defined in Chapter IV, a bar placed over the variables is used to designate the concentrated moment problem. Thus equation (88) is rewritten as:

$$\bar{W}_1 = \frac{M}{8\pi} (\bar{A}\rho + \bar{B}\rho^3 + \bar{C}\rho^{-1} + \bar{F}\rho \ln \rho) \cos \theta \quad (89)$$

where:

$$\begin{aligned} \bar{A} &= -1 \\ \bar{B} &= 1 \\ \bar{C} &= -\beta^2 = 0 \\ \bar{F} &= -2 \end{aligned} \quad (90)$$

Due to the presence of the  $\rho \ln \rho$  term in equation (89), the slope and bending stresses will become infinite at the origin. The expressions for the linear small-deflection stress resultants can be obtained from equations (44) by substituting the product of  $(M/8\pi)$  and the barred constants for the product of  $\alpha$  and the unbarred constants (i.e.,  $A\alpha = \bar{A}M/8\pi$ ).

The governing equation for the stress function is obtained from equation (48) by making the substitutions for constants mentioned above.

Substituting for the unbarred constants in equation (50) gives the following solution for the stress function:

$$\begin{aligned} \bar{\varphi}_2 = & - 12 (1-\nu^2) \lambda^2 \left( \frac{M}{8\pi} \right)^2 \left[ \bar{B}_0 \rho^2 + \bar{C}_0 \ln \rho + \bar{D}_0 \rho^2 \ln \rho \right. \\ & + \frac{\rho^4}{146} (\rho^2 - 9) + \cos 2\theta \left[ \bar{A}_2 \rho^2 + \bar{B}_2 \rho^{-2} + \bar{C}_2 \rho^4 + \bar{D}_2 \right. \\ & \left. \left. + \frac{\rho^2}{48} (\rho^4 - 12 (1 + \rho^2) \ln \rho) \right] \right] \end{aligned} \quad (91)$$

From equation (61), the constant  $\bar{D}_0$  must be:

$$\bar{D}_0 = 1/4 \quad (92)$$

in order to eliminate multi-valued in-plane displacements. By letting  $\beta$  equal zero and making the substitution for the constants A, B, C, F as mentioned previously, equations (65) reduce to the following expressions for the constants of integration in equation (91):

$$\begin{aligned} \bar{B}_0 &= \frac{\nu - 5}{48(1 - \nu)} \\ \bar{C}_0 &= 0 \\ \bar{A}_2 &= \frac{9\nu - 7}{48(1 + \nu)} \\ \bar{B}_2 &= 0 \\ \bar{C}_2 &= \frac{13 - 5\nu}{24(3 - \nu)} \\ \bar{D}_2 &= 0 \end{aligned} \quad (93)$$

The vanishing of  $\bar{C}_0$ ,  $\bar{B}_2$  and  $\bar{D}_2$  could have been ascertained without going through the algebra used to obtain equations (93), because if they are not zero the in-plane displacements would be infinite at the center of the plate. However, the  $\rho^2 \ln \rho$  term in equation (91) causes the membrane stress resultants to become infinite at the origin. Expressions for the in-plane displacements and stress resultants can be obtained from equations (59), (60) and (67) by making the substitutions mentioned previously for A, B, C and F and by replacing the product of  $\alpha^2$  and the unbarred constants given in equations (65) with the product of  $(M/8\pi)^2$  and the corresponding barred constants in equation (93).

The governing equation for the second approximation to the lateral displacement is obtained from equation (69) by making the substitutions for the unbarred constants mentioned in the preceding paragraph. Making the same substitutions in equation (72) gives the following expression for the second approximation to the lateral displacement:

$$\begin{aligned} \bar{W} = & \bar{W}_1 - 12 (1-\nu^2) \lambda^2 \left( \frac{M}{8\pi} \right)^3 \left[ (\bar{A}_1 \rho + \bar{B}_1 \rho^3 + \bar{C}_1 \rho^{-1} \right. \\ & + \bar{D}_1 \rho \ln \rho + \bar{R}_{10} \rho^9 + \bar{R}_{11} \rho^7 + \bar{R}_{12} \rho^5 + \bar{R}_{13} \rho^5 \ln \rho \\ & \left. + \bar{R}_{14} \rho^3 \ln \rho + \bar{R}_{15} \rho^3 \ln^2 \rho) \cos \theta + \right. \end{aligned}$$

$$\begin{aligned}
 & + (\bar{A}_3 \rho^3 + \bar{B}_3 \rho^{-3} + \bar{C}_3 \rho^5 + \bar{D}_3 \rho^{-1} + \bar{R}_{20} \rho^9 \\
 & + \bar{R}_{21} \rho^7 + \bar{R}_{22} \rho^7 \ln \rho + \bar{R}_{23} \rho^5 \ln \rho + \bar{R}_{24} \rho^5 \ln^2 \rho \\
 & + \bar{R}_{25} \rho^3 \ln \rho + \bar{R}_{26} \rho^3 \ln^2 \rho) \cos 3\theta \quad (94)
 \end{aligned}$$

where  $\bar{W}_1$  is given in equation (89) and where:

$$\begin{aligned}
 \bar{R}_{10} &= -1/3,840 \\
 \bar{R}_{11} &= 7/1,536 \\
 \bar{R}_{12} &= (3 + 6\nu - 5\nu^2)/288(1 - \nu^2) \\
 \bar{R}_{13} &= -1/32 \\
 \bar{R}_{14} &= -(3 + 3\nu - 4\nu^2)/24(1 - \nu^2) \\
 \bar{R}_{15} &= 3/32 \\
 \bar{R}_{20} &= -7/17,280 \\
 \bar{R}_{21} &= -(126 - 47\nu)/4,800(3 - \nu) \\
 \bar{R}_{22} &= 3/320 \\
 \bar{R}_{23} &= (103 - 37\nu)/284(3 - \nu) \\
 \bar{R}_{24} &= -1/64 \\
 \bar{R}_{25} &= (2 + \nu)/36(1 + \nu) \\
 \bar{R}_{26} &= 1/96 \quad (95)
 \end{aligned}$$

By letting  $\beta = 0$  and substituting the barred constants from equation (95) for the corresponding unbarred constants in equations (74) and (76) (the constants  $\bar{R}_{16}$ ,  $\bar{R}_{17}$ ,  $\bar{R}_{18}$ ,  $\bar{R}_{19}$ ,  $\bar{R}_{27}$ ,  $\bar{R}_{28}$  and  $\bar{R}_{29}$  are zero), the following expressions for the constants of integration in equation (94) are obtained:

$$\begin{aligned}\bar{A}_1 &= - (657 + 480\nu - 817 \nu^2)/11,520 (1 - \nu^2) \\ \bar{B}_1 &= (1029 + 480 \nu - 1189 \nu^2)/23,040 (1 - \nu^2) \\ \bar{C}_1 &= 0 \\ \bar{D}_1 &= 0 \\ \bar{A}_3 &= 1/2 [7\bar{R}_{20} + 5\bar{R}_{21} + \bar{R}_{22} + \bar{R}_{23} + \bar{R}_{25}] \\ \bar{B}_3 &= 0 \\ \bar{C}_3 &= - 1/2 [6\bar{R}_{20} + 4\bar{R}_{21} + \bar{R}_{22} + \bar{R}_{23} + \bar{R}_{25}] \\ \bar{D}_3 &= 0\end{aligned}\tag{96}$$

The expressions for the bending stress resultants from the iteration solution can be obtained from equations (79) by substituting the product of  $(M/8\pi)^3$  and the barred constants for the product of  $\alpha^3$  and the corresponding unbarred constants.

#### B. Discussion.

Since the stresses and slopes become infinite at the origin for both linear and nonlinear theories, a plot of these quantities is

awkward. However, the nonlinear effect can be seen from the plot of maximum lateral displacement versus applied moment as given in Figure 18. In order to compare the concentrated moment solution with that for the case of a very small rigid inclusion, numerical values for  $\beta = 0.01$  are also shown in Figure 18.



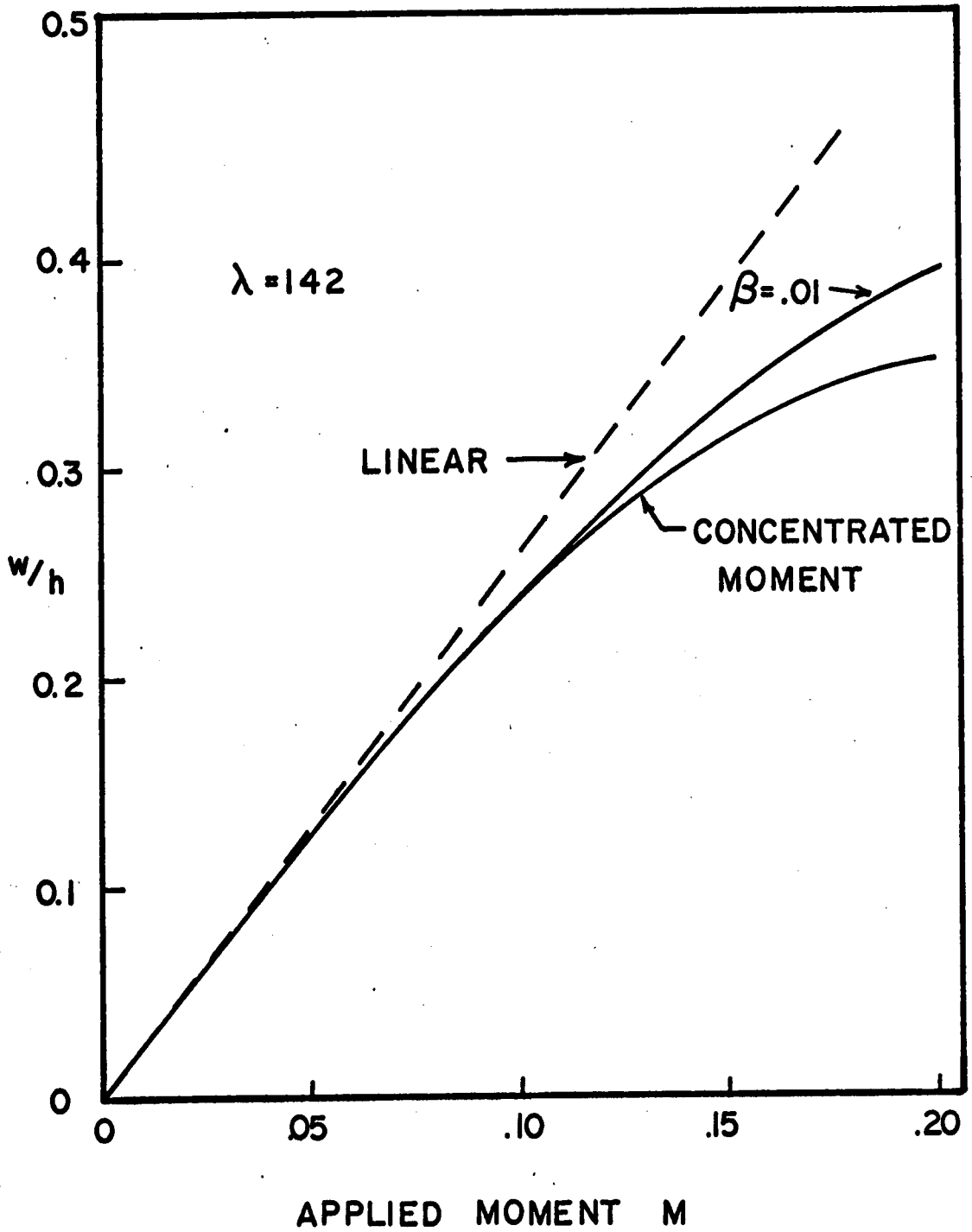


FIGURE 18. Maximum lateral displacement for concentrated moment

## VII. EXTENSION OF THE PROBLEM

A brief discussion of a preliminary investigation into another interesting method of solving the title problem of this dissertation is given in Section A of this chapter. To further illustrate the boundary layer phenomenon mentioned in Chapter IV, the case where the annular plate is subjected to a large initial prestress is discussed in Section B.

### A. Series Truncation.

The series truncation method has been used successfully to solve various nonlinear fluid mechanics problems. In brief the method involves assuming a solution as a series expanded in terms of one of the independent variables, where the coefficients of the series are unspecified functions of the other independent variables. The series is truncated after a certain number of terms and the effect of the truncation is evaluated by comparing the solution resulting from an (n) term series to that obtained from an (n + 1) term series. However, the labor of solution increases greatly with the number of terms in the series.

Results from the fluid mechanics investigations (see reference 20) show that a careful selection of the expansion coordinate greatly improves the solution. For the problem in this investigation, since

one would expect the most predominant variation in deflections to be in the radial direction, the azimuthal coordinate is the logical selection for the expansion coordinate.

Using the iteration solution as a guide, although this is by no means a prerequisite for the series truncation method, one possible form for the assumed series which is very similar to the Levy type of solution is:

$$W(\rho, \theta) = W_0(\rho) \cos \theta + W_1(\rho) \cos 3\theta + \dots \quad (97)$$

$$\varphi(\rho, \theta) = \varphi_0(\rho) + \varphi_1(\rho) \cos 2\theta + \dots \quad (98)$$

Upon substitution of equations (97) and (98) into the two von Karman equations (eqs. 13 and 20), and collecting coefficients of the different trigonometric functions of  $\theta$ , a set of nonlinear ordinary differential equations for the series coefficients are obtained.

However, the stress function is no longer a convenience to the solution because a numerical integration technique of some sort would be used to solve the nonlinear equations and the boundary conditions are prescribed on the displacements.

The von Karman equations can easily be written in terms of the displacements (simply by not introducing the stress function in Chapter III). With the governing equations written in terms of the displacements, in addition to the assumed form for  $W$  in equation (97), the solutions for the in-plane displacements can be assumed as:

$$U(\rho, \theta) = U_0(\rho) + U_1(\rho) \cos 2\theta + \dots \quad (99)$$

$$V(\rho, \theta) = V_0(\rho) \sin 2\theta + V_1(\rho) \sin 4\theta + \dots \quad (100)$$

Substitution of equations (97), (99) and (100) into the von Karman equations (written in terms of displacements) results in a set of nonlinear ordinary differential equations for the series coefficients  $W_0, U_0, V_0$ , etc. The difficulty of the numerical solution to these equations is increased by the fact that boundary conditions are specified at both the inner and outer boundaries.

A more recent series truncation method, referred to as the "local truncation," assumes the solution as a series expanded in powers of one coordinate about an arbitrary value of that coordinate and the coefficients of the series are unspecified functions of the other coordinate. Using the iteration solution as a guide, a solution to the von Karman equations can be assumed as a power series in  $\theta$  about some arbitrary angle  $\theta_0$  in the following form:

$$W(\rho, \theta) = \cos \theta \left[ W_0(\rho) + \delta W_1(\rho) + \delta^2 W_2(\rho) + \dots \right] \quad (101)$$

$$U(\rho, \theta) = U_0(\rho) + \delta U_1(\rho) + \delta^2 U_2(\rho) + \dots \quad (102)$$

$$V(\rho, \theta) = \sin 2\theta \left[ V_0(\rho) + \delta V_1(\rho) + \delta^2 V_2(\rho) + \dots \right] \quad (103)$$

where  $\delta = \theta - \theta_0$ . When equations (101), (102), (103) are substituted into the governing equations, nonlinear ordinary differential equations for the series coefficients are obtained.

Without actually carrying out numerical calculations, it is difficult to predict which series truncation method would give the best results.

B. Large Initial Prestress.

As was mentioned in Section C of Chapter IV, for fairly large deflections, a plate behaves as a membrane except in regions very close to the boundaries. The study of such a problem becomes quite involved, however the same phenomenon occurs in the much simpler case of large initial prestress. If the plate is subjected to a large uniform initial prestress so that the dimensionless in-plane stress resultants have the value  $T$  (i.e.,  $N_r = N_\theta = T$ ,  $N_{r\theta} = 0$ ) before the rigid inclusion is rotated, then any subsequent lateral displacement will not significantly change the in-plane forces and they will remain constant. Since the in-plane forces remain constant, the in-plane equilibrium equations (eqs. 1 and 2) are automatically satisfied. The governing equations then reduce to one, linear partial differential equation for the lateral displacement, which is obtained from equation (20) by introducing the constant  $T$  for the dimensionless in-plane stress resultants. The resulting equation is:

$$\nabla^4 W = T \nabla^2 W \quad (104)$$

where  $\nabla^2$  is the Laplacian operator, which for cylindrical coordinates

is  $(\nabla^2 = \frac{\partial^2}{\partial \rho^2} + \frac{1}{\rho} \frac{\partial}{\partial \rho} + \frac{1}{\rho^2} \frac{\partial^2}{\partial \theta^2})$  .

From the boundary conditions (eqs. 34, 35, 38 and 39), the solution is assumed in the form:

$$W(\rho, \theta) = W^*(\rho) \cos \theta \quad (105)$$

and substituting equation (105) into equation (104) gives the following governing equation for  $W^*$ :

$$\left[ \frac{d^2}{d\rho^2} + \frac{1}{\rho} \frac{d}{d\rho} - \frac{1}{\rho^2} - T \right] \left[ \frac{d^2 W^*}{d\rho^2} + \frac{1}{\rho} \frac{dW^*}{d\rho} - \frac{W^*}{\rho^2} \right] = 0 \quad (106)$$

For very large  $T$ , the first three terms of the first operator in equation (106) are negligible and the governing equation for  $W^*$  reduces to the following second order equation:

$$\frac{d^2 W^*}{d\rho^2} + \frac{1}{\rho} \frac{dW^*}{d\rho} - \frac{W^*}{\rho^2} = 0 \quad (107)$$

However, four boundary conditions are prescribed on the lateral displacement, therefore equation (107) is over-specified since it is only of second order. Obviously two boundary conditions have been lost, and the question is which two should be satisfied. This mystery is explained by the fact that equation (107) is actually the membrane equation and only displacements can be specified for the membrane. In order to satisfy the slope boundary conditions, the regions near the boundary must be examined in more detail. For this brief discussion, only the inner boundary is treated in detail, however, the outer boundary can be handled in the same way.

An exact solution to equation (106) can probably be found in terms of Bessel Functions, however it is informative to develop the solution by perturbation methods. The perturbation procedure used in this section is the method of inner and outer expansions, which is discussed in detail in Chapter V of reference 19.

Selecting a small parameter  $t$  such that:

$$t^2 = 1/T \quad (108)$$

where  $T$  is the large dimensionless membrane stress resultant, the solution for  $W^*$  is assumed in the form:

$$W^* = W_0^* + t W_1^* + t^2 W_2^* + \dots \quad (109)$$

The matching principle will verify that the form of the expansion in equation (109) is correct.

To magnify the region near the inner boundary, a new boundary layer coordinate  $\xi$  is introduced as:

$$\rho = \beta + t \xi \quad (110)$$

Thus for small  $t$ ,  $\xi$  will still be of order (1) when  $\rho$  is very close to  $\beta$ . Equation (106) rewritten in terms of  $t$  is:

$$\left[ 1 - t^2 \left( \frac{d^2}{d\rho^2} + \frac{1}{\rho} \frac{d}{d\rho} - \frac{1}{\rho^2} \right) \right] \left[ \frac{d^2 W^*}{d\rho^2} + \frac{1}{\rho} \frac{dW^*}{d\rho} - \frac{W^*}{\rho^2} \right] = 0 \quad (111)$$

and transforming equation (111) into the boundary layer coordinates gives:

$$\left[ 1 - \frac{d^2}{d\xi^2} - \frac{t}{(\beta + t\xi)} \frac{d}{d\xi} + \frac{t^2}{(\beta + t\xi)^2} \right] \left[ \frac{d^2 W^*}{d\xi^2} + \frac{t}{(\beta + t\xi)} \frac{dW^*}{d\xi} - \frac{t^2 W^*}{(\beta + t\xi)^2} \right] = 0 \quad (112)$$

where  $W^*$  in equation (112) is a function of  $\xi$ .

Equation (111) is the governing equation in the middle portion of the plate (referred to as the outer region) and equation (112) is the governing equation in the boundary layer near the rigid inclusion (referred to as the inner region).

Substituting the first two terms of the assumed solution (eq. 109) into equation (111) and collecting powers of  $t$  gives the following governing equations in the outer region :

$$t^0: \quad \frac{d^2 W_0^*}{d\rho^2} + \frac{1}{\rho} \frac{dW_0^*}{d\rho} - \frac{W_0^*}{\rho^2} = 0 \quad (113)$$

$$t^1: \quad \frac{d^2 W_1^*}{d\rho^2} + \frac{1}{\rho} \frac{dW_1^*}{d\rho} - \frac{W_1^*}{\rho^2} = 0 \quad (114)$$

In this discussion, only the solutions to order ( $t$ ) will be obtained, however higher order approximations can be obtained in the same manner by keeping more terms in the assumed solution. For the first approximation, the effect of the boundary layer is so small that the displacement boundary conditions given by equations (34) and (38) are



assumed to hold in the outer region. This assumption is substantiated later by the matching principle.

The solution to equation (113) is:

$$W_o^* = E_1 \rho + E_2 \rho^{-1} \quad (115)$$

and using the boundary conditions (eqs. 34 and 38) to solve for the constants of integration, equation (115) becomes:

$$W_o^* = - \frac{\beta^2 \alpha}{1 - \beta^2} (\rho - \rho^{-1}) \quad (116)$$

The solution to equation (114) is:

$$W_1^* = E_3 \rho + E_4 \rho^{-1} \quad (117)$$

where  $E_3$  and  $E_4$  are constants of integration which will be determined from the matching principle. Thus the two-term solution for the lateral displacement from equations (109), (116) and (117) is:

$$W^* = - \frac{\beta^2 \alpha}{1 - \beta^2} (\rho - \rho^{-1}) + t(E_3 \rho + E_4 \rho^{-1}) \quad (118)$$

Substituting the assumed form for  $W^*$  as given in equation (109) into equation (112) and placing a bar over  $W^*$  to indicate the inner region, the following equations are obtained by collecting powers of  $t$ :

$$t^0: \quad \frac{d^2}{d\xi^2} \left[ \frac{d^2 \bar{W}_0^*}{d\xi^2} - \bar{W}_0^* \right] = 0 \quad (119)$$

$$t^1: \quad \frac{d^2}{d\xi^2} \left[ \frac{d^2 \bar{W}_1^*}{d\xi^2} - \bar{W}_1^* \right] = -\frac{1}{\beta} \left[ 2 \frac{d^3 \bar{W}_0^*}{d\xi^3} - \frac{d\bar{W}_0^*}{d\xi} \right] \quad (120)$$

The solution to equation (119) is:

$$\bar{W}_0^* = E_5 e^{\xi} + E_6 e^{-\xi} + E_7 \xi + E_8 \quad (121)$$

The boundary conditions for the inner solution are obtained by writing equations (34) and (35) in terms of the inner variable and noting that at  $\rho = \beta$ ,  $\xi$  is zero. The boundary conditions for  $\xi = 0$  are:

$$\bar{W} = \beta \alpha$$

$$\frac{d\bar{W}^*}{d\xi} = t \alpha \quad (122)$$

or in terms of  $\bar{W}_0^*$  and  $\bar{W}_1^*$  equations (122) become:

$$\bar{W}_0^* = \beta \alpha$$

$$\frac{d\bar{W}_0^*}{d\xi} = 0 \quad (123)$$

and:

$$\bar{W}_1^* = 0$$

$$\frac{d\bar{W}_1^*}{d\xi} = \alpha \quad (124)$$

For very large  $\xi$  (which corresponds to points in the middle region of the plate), the first term in equation (121) becomes exponentially large and therefore  $E_5$  must vanish. The vanishing of  $E_5$  would also be required by the matching principle. Using the boundary conditions as given in equations (123) and using the matching principle to match  $W_0^*$  and  $\bar{W}_0^*$ , the following expressions for the remaining constants in equation (121) are obtained:

$$\begin{aligned} E_6 &= E_7 = 0 \\ E_8 &= \beta \alpha \end{aligned} \tag{125}$$

Thus equation (121) becomes:

$$\bar{W}_0^* = \beta \alpha \tag{126}$$

Since  $\bar{W}_0^*$  is a constant, its derivatives in equation (120) vanish and the solution for  $\bar{W}_1^*$  is:

$$\bar{W}_1^* = E_9 e^{\xi} + E_{10} e^{-\xi} + E_{11} \xi + E_{12} \tag{127}$$

The leading term in equation (127) becomes exponentially large for large  $\xi$  and therefore  $E_9$  must vanish. Using the boundary conditions given in equation (124) and the matching principle to match  $W_1^*$  and  $\bar{W}_1^*$ , the following expressions for the remaining constants in equation (127) are obtained:

$$E_{10} = - \frac{2\alpha}{1 - \beta^2}$$

$$E_{11} = - \frac{(1 + \beta^2) \alpha}{1 - \beta^2}$$

$$E_{12} = \frac{2\alpha}{1 - \beta^2} \tag{128}$$

and also the following condition for the constants in equation (118):

$$\beta^2 E_3 + E_4 = \frac{2\beta \alpha}{1 - \beta^2} \tag{129}$$

Combining equations (109), (126), (127) and (128), the two-term inner equation for the lateral displacement is:

$$\bar{w}^* = \beta \alpha - \frac{\tau\alpha}{1-\beta^2} \left[ \xi(1+\beta^2) + 2(e^{-\xi}-1) \right] \tag{130}$$

Only one relationship for the two undetermined constants in equation (118) is obtained by the above matching, however a similar condition to equation (129) results from matching the two-term outer solution to a two-term boundary layer solution for the outer edge of the plate.

Only the results of developing a two-term expansion for the outer boundary layer are given here because the procedure is very similar to that for the inner boundary layer. Upon introducing an outer

boundary layer coordinate  $\eta$  defined by:

$$\rho = 1 - t \eta \quad (131)$$

and following the development used for the inner boundary layer, the other expression needed to solve for the constants in equation (118) is found to be:

$$E_3 + E_4 = - \frac{2 \beta^2 \alpha}{1 - \beta^2} \quad (132)$$

Solving for  $E_3$  and  $E_4$  from equations (129) and (132) and substituting them into equation (118), the expression for the two-term outer expansion is obtained. The results are summarized in the three equations below where the bar notation has been discontinued:

Inner boundary layer

$$W^* = \beta \alpha - \frac{t \alpha}{1 - \beta^2} \left[ \xi (1 + \beta^2) + 2(e^{-\xi} - 1) \right] \quad (133)$$

Central region

$$W^* = - \frac{\beta^2 \alpha}{1 - \beta^2} (\rho - \rho^{-1}) + \frac{2\beta \alpha t}{(1 - \beta^2)^2} \left[ (1 + \beta^3) \rho^{-1} - (1 + \beta) \rho \right] \quad (134)$$

Outer boundary layer

$$W^* = \frac{2\beta^2 \alpha t}{1 - \beta^2} \left[ e^{-\eta} + \eta - 1 \right] \quad (135)$$

VIII. ACKNOWLEDGMENTS

The author wishes to express his sincere thanks to his advisor, Dr. R. T. Davis, for suggesting the topic and for his invaluable guidance, encouragement and enthusiasm throughout this study. He also expresses his gratitude to the members of his graduate committee, Professors G. A. Gray, C. B. Ling, A. A. Pap and G. W. Swift for their criticisms of this work. A special thank you to Professor D. H. Pletta for his assistance in obtaining financial support for the experimental part of this investigation, the computer work and particularly the opportunity for the author to present part of this work at the Fifth U. S. National Congress of Applied Mechanics. It has been a privilege to study under and to be associated with the faculty at Virginia Polytechnic Institute.

Thanks are extended to \_\_\_\_\_ and \_\_\_\_\_ for helping with the experiments, to \_\_\_\_\_ for helping "debug" part of the analytical work, to \_\_\_\_\_ for preparation of some of the figures, and to \_\_\_\_\_ for typing the manuscript.

Most of all, the author wishes to thank his wife, \_\_\_\_\_, for her constant help and understanding throughout this investigation and during our eight years of college.

IX. BIBLIOGRAPHY

1. Chien, W. Z., Large Deflection of a Circular Clamped Plate Under Uniform Pressure, Chinese Journal of Physics, Vol. 7, 1947, pp. 102-113.
2. Davis, R. T., Lectures on Perturbation Methods in Mechanics, Engineering Mechanics Department, Virginia Polytechnic Institute, 1966 (unpublished).
3. Fung, Y. C., Foundations of Solid Mechanics, Prentice-Hall, Englewood Cliffs, New Jersey, 1965, pp. 463-470.
4. Hamada, M., On the Accuracy of the von Karman Equations for Axisymmetric Non-Linear Bending for Circular Plates, Japan Society for Aeronautical and Space Sciences, Trans. Vol. 8, No. 12, 1965, pp. 6-14.
5. Hamada, M. and Seguchi, Y., Large Deflection Analysis of Circular Ring Plates under Uniform Transverse Force Along the Inner Edge, Bull. of Japan Society of Mechanical Engineers, Vol. 8, No. 31, 1965, pp. 344-352.
6. Hart, V. G. and Evans, D. J., Non-Linear Bending of an Annular Plate by Transverse Edge Forces, Journal of Mathematics and Physics, Vol. 43, 1964, pp. 275-303.
7. Koehli, A. and Evan-Iwanowski, R. M., Combined Effect of Rotation and Edge Force on Large Deflections of Thin Annular Plates,

Developments in Theoretical and Applied Mechanics, Vol. 1,  
Proc. of First Southeastern Conference on Theoretical and Applied  
Mechanics, Plenum Press, New York, 1963, pp. 191-205.

8. Liberty, J. and Collier, J., Experimental Investigation of  
Unsymmetric Large Deflections of an Annular Plate, Senior  
Project, Engineering Mechanics Department, Virginia Polytechnic  
Institute, 1966.
9. P'an Li-Chou, Large Deflection of a Circular Clamped Plate Under  
a Linearly Varying Load, Li-hsueh Hsueh-pao (Journal of  
Mechanics), Peiping, Vol. 1, No. 2, 1957, pp. 205-232, (trans-  
lation distributed by Office of Technical Services, JPRS 11480,  
Dec. 1961).
10. Reissner, E., On Finite Twisting and Bending of Circular Ring  
Sector Plates and Shallow Helicoidal Shells, Quarterly of  
Applied Mathematics, Vol. 11, No. 4, 1954, pp. 473-483.
11. Reissner, E., Rotationally Symmetric Problems in the Theory of  
Thin Elastic Shells, Proc. of Third U. S. National Congress  
of Applied Mechanics, 1958, pp. 51-69.
12. Reissner, E., Unsymmetrical Nonlinear Bending of Thin Plates,  
Third Southeastern Conference on Theoretical and Applied  
Mechanics, March 31-April 1, 1966, Columbia, South Carolina,  
(Proceedings to appear).



13. Reissner, H., Über die unsymmetrische Biegung dünner Kreisringplatten, Ingr. - Arch., Vol. 1 1930, pp. 72-83.
14. Roark, R. J., Stresses Produced in a Circular Plate by Eccentric Loading and by a Transverse Couple, Bull. of the Univ. of Wisconsin, Engr. Experiment Station Series, No. 74, 1932.
15. Sliter, G. E., Nikolai, R. J., and Boresi, A. P., Elastic Plates: Annotated Bibliography 1930-1962, Univ. of Illinois, Engr. Experiment Station, Technical Report 10, 1963.
16. Sherbourne, A. N. and Lennox, W. C., Elastic, Large Deflections of Annular Membranes, Journal of Engineering Mechanics Division, American Society of Civil Engineers, Vol. 92, No. EM 2, 1966, pp. 75-99.
17. Tamate, O. and Abe, H., Large Deflections of Annular Plates Under Uniform Pressure with Outer Edge Clamped and Inner Edge Free, Technology Reports, Tohoku University, Vol. 29, No. 1, 1964, pp. 39-53.
18. Timoshenko, S. and Woinowsky-Krieger, S., Theory of Plates and Shells, McGraw Hill, New York, Second Edition, 1959.
19. Van Dyke, M., Perturbation Methods in Fluid Mechanics, Academic Press, New York, 1964.

20. Van Dyke, M., The Circle at Low Reynolds Number as a Test of the Method of Series Truncation, Stanford University, SUDAER Report No. 211, October 1964.
21. Vol'mir, A. S., Survey of Investigations on the Theory of Flexible Plates and Shells (covering the period from 1941 to 1957), NASA Technical Translation, No. F - 180, 1963.
22. Way, S., Bending of Circular Plates with Large Deflection, Trans. of American Society of Mechanical Engineers, Vol. 56, 1934, pp. 627-636.
23. Wempner, G. A. and Schmidt, R., Large Symmetric Deflections of Annular Plates, Journal of Applied Mechanics, Vol. 25, 1958, pp. 449-452.

**The vita has been removed from  
the scanned document**

APPENDIX A

Derivation of von Karman Equations from  
Equations of Elasticity

In this section the von Karman equations are derived by using the equations of finite elasticity and incorporating the assumptions of large deflection plate theory given in Chapter III. This derivation follows Fung (3) very closely and is included here only to further point out the use of the Lagrangian description in the von Karman equations. In discussing the von Karman equations on page 469 of his text, Fung says,

"These equations were given without proof by von Karman in 1910. Most books give derivations of these equations without a clear indication as to whether Lagrangian or Eulerian descriptions are used. The explicit use of Lagrangian description introduces a degree of clarity not hitherto achieved."

The notation used throughout this derivation is:

- $x, y, z$  rectangular cartesian coordinates
- $u_x, u_y, u_z$  displacements of a point in the plate in the  $x, y, z$  directions respectively
- $U, V, W$  displacements of the plate middle surface in the  $x, y, z$  directions respectively
- , subscripts following the comma denote partial derivative with respect to that coordinate.

$$\nabla^4 = \left( \frac{\partial^4}{\partial x^4} + 2 \frac{\partial^4}{\partial x^2 \partial y^2} + \frac{\partial^4}{\partial y^4} \right)$$

$$L(W, \varphi) = \left( \frac{\partial^2 W}{\partial x^2} \frac{\partial^2 \varphi}{\partial y^2} - 2 \frac{\partial^2 W}{\partial x \partial y} \frac{\partial^2 \varphi}{\partial x \partial y} + \frac{\partial^2 W}{\partial y^2} \frac{\partial^2 \varphi}{\partial x^2} \right)$$

For plate theory, all but three strain components are neglected. The three remaining strain components from the Green Strain tensor, which is based on the Lagrangian description, are:

$$\begin{aligned} E_{xx} &= u_{x,x} + \frac{1}{2} \left[ (u_{x,x})^2 + (u_{y,x})^2 + (u_{z,x})^2 \right] \\ E_{yy} &= u_{y,y} + \frac{1}{2} \left[ (u_{x,y})^2 + (u_{y,y})^2 + (u_{z,y})^2 \right] \\ E_{xy} &= \frac{1}{2} \left[ u_{x,y} + u_{y,x} + u_{x,x} u_{x,y} + u_{y,x} u_{y,y} \right. \\ &\quad \left. + u_{z,x} u_{z,y} \right] \end{aligned} \tag{A1}$$

According to the assumptions of plate theory, the displacements of a point located a distance  $z$  from the middle surface can be written as:

$$\begin{aligned} u_x &= U - z W_{,x} \\ u_y &= V - z W_{,y} \\ u_z &= W \end{aligned} \tag{A2}$$

where  $U$ ,  $V$  and  $W$  are the displacements of the middle surface.

Neglecting the nonlinear terms in equations (A1) which involve the in-plane displacements and substituting from equations (A2), equations (A1) reduce to:

$$\begin{aligned} E_{xx} &= U_{,x} - z W_{,xx} + \frac{1}{2} (W_{,x})^2 \\ E_{yy} &= V_{,y} - z W_{,yy} + \frac{1}{2} (W_{,y})^2 \\ E_{xy} &= \frac{1}{2} (U_{,y} + V_{,x} - 2z W_{,xy} + W_{,x} W_{,y}) \end{aligned} \quad (A3)$$

A compatibility equation found from equations (A3) is:

$$E_{xx,yy} + E_{yy,xx} - 2E_{xy,xy} = (W_{,x y})^2 - W_{,xx} W_{,yy} \quad (A4)$$

Using Hooke's Law, the expressions for the stresses found from equations (A3) are:

$$\begin{aligned} S_{xx} &= \frac{E}{1 - \nu^2} (E_{xx} + \nu E_{yy}) \\ &= \frac{E}{1 - \nu^2} \left[ U_{,x} + \nu V_{,y} - z(W_{,xx} + \nu W_{,yy}) \right. \\ &\quad \left. + \frac{1}{2} (W_{,x})^2 + \frac{\nu}{2} (W_{,y})^2 \right] \\ S_{yy} &= \frac{E}{1 - \nu^2} (E_{yy} + \nu E_{xx}) \\ &= \frac{E}{1 - \nu^2} \left[ V_{,y} + \nu U_{,x} - z(W_{,yy} + \nu W_{,xx}) \right. \\ &\quad \left. + \frac{1}{2} (W_{,y})^2 + \frac{\nu}{2} (W_{,x})^2 \right] \end{aligned}$$

$$\begin{aligned}
 S_{xy} &= \frac{E}{1+\nu} E_{xy} \\
 &= \frac{E}{2(1+\nu)} \left[ U_{,y} + V_{,x} - 2z W_{,xy} + W_{,x} W_{,y} \right] \quad (A5)
 \end{aligned}$$

Using the definitions of the in-plane stress resultants:

$$N_x = \int_{-h/2}^{h/2} S_{xx} dz \quad N_y = \int_{-h/2}^{h/2} S_{yy} dz \quad N_{xy} = \int_{-h/2}^{h/2} S_{xy} dz \quad (A6)$$

and multiplying equations (A5) by dz and integrating from - h/2 to h/2, the following expressions for the stress resultants are obtained:

$$\begin{aligned}
 N_x &= \frac{Eh}{1-\nu^2} \left[ U_{,x} + \nu V_{,y} + \frac{1}{2} (W_{,x})^2 + \frac{\nu}{2} (W_{,y})^2 \right] \\
 N_y &= \frac{Eh}{1-\nu^2} \left[ V_{,y} + \nu U_{,x} + \frac{1}{2} (W_{,y})^2 + \frac{\nu}{2} (W_{,x})^2 \right] \\
 N_{xy} &= \frac{Eh}{2(1+\nu)} \left[ U_{,y} + V_{,x} + W_{,x} W_{,y} \right] \quad (A7)
 \end{aligned}$$

By multiplying equations (A5) by zdz and integrating from - h/2 to h/2 and using the definition of the moment resultants:

$$M_x = \int_{-h/2}^{h/2} S_{xx} zdz \quad M_y = \int_{-h/2}^{h/2} S_{yy} zdz \quad M_{xy} = \int_{-h/2}^{h/2} S_{xy} zdz \quad (A8)$$

the following expressions for the moment resultants are obtained:

$$\begin{aligned}
 M_x &= -D (W_{,xx} + \nu W_{,yy}) \\
 M_y &= -D (W_{,yy} + \nu W_{,xx}) \\
 M_{xy} &= -(1 - \nu) D W_{,xy}
 \end{aligned} \tag{A9}$$

where D is the plate stiffness.

The equilibrium equations, in the Lagrangian description are:

$$\left[ S_{jk} (\delta_{ik} + u_{i,k}) \right]_{,j} + \bar{X}_i = 0 \tag{A10}$$

where  $\delta_{ik}$  is the Kronecker delta, i is a range index, j and k are summation indexes, and  $\bar{X}_i$  is the body force. Expanding equation (A10) and neglecting body forces and higher order terms, the equilibrium equations become:

$$S_{xx,x} + S_{xy,y} + S_{xz,z} = 0 \tag{A11}$$

$$S_{xy,x} + S_{yy,y} + S_{yz,z} = 0 \tag{A12}$$

$$\begin{aligned}
 (S_{xx} W_{,x} + S_{xy} W_{,y} + S_{xz})_{,x} + (S_{yx} W_{,x} + \\
 S_{yy} W_{,y} + S_{yz})_{,y} + (S_{xz} W_{,x} + S_{yz} W_{,y} + S_{zz})_{,z} = 0
 \end{aligned} \tag{A13}$$

Multiplying equations (A11) and (A12) by dz and integrating from -h/2 to h/2 yields:

$$\begin{aligned}
 N_{x,x} + N_{xy,y} &= 0 \\
 N_{xy,x} + N_{y,y} &= 0
 \end{aligned} \tag{A14}$$



and multiplying them by  $zdz$  and integrating from  $-h/2$  to  $h/2$  gives:

$$\begin{aligned} M_{x,x} + M_{xy,y} &= Q_x \\ M_{xy,x} + M_{y,y} &= Q_y \end{aligned} \tag{A15}$$

where the shear resultants  $Q_x$  and  $Q_y$  are defined by:

$$Q_x = \int_{-h/2}^{h/2} S_{xz} dz \quad Q_y = \int_{-h/2}^{h/2} S_{yz} dz \tag{A16}$$

Multiplying equation (A13) by  $dz$  and integrating from  $-h/2$  to  $h/2$  gives:

$$(Q_x + N_x W_{,x} + N_{xy} W_{,y})_{,x} + (Q_y + N_{xy} W_{,x} + N_y W_{,y})_{,y} = 0 \tag{A17}$$

In evaluating the limits on the integrals used to obtain equations (A14), (A15), and (A17), the stresses on the upper and lower surfaces of the plate are assumed to be zero (i.e., no surface loading).

Combining equations (A15) and (A17) results in:

$$M_{x,xx} + 2M_{xy,xy} + M_{y,yy} = - [N_x W_{,xx} + 2N_{xy} W_{,xy} + N_y W_{,yy}] \tag{A18}$$

and combining equations (A18) and (A9) gives:

$$D \nabla^4 W = N_x W_{,xx} + 2N_{xy} W_{,xy} + N_y W_{,yy} \tag{A19}$$

The stress function  $\varphi$ , which is defined so as to satisfy the in-plane equilibrium equations (eqs. A14) exactly, is given by:

$$N_x = \varphi,_{yy} \qquad N_y = \varphi,_{xx} \qquad N_{xy} = -\varphi,_{xy} \qquad (A20)$$

Solving for the strains in terms of the stress function and substituting into the compatibility equation (eq. A4), the first von Karman equation is obtained:

$$\nabla^4 \varphi = -\frac{Eh}{2} L(W,W) \qquad (A21)$$

where  $L(W,W)$  is obtained from the expression for  $L(W,\varphi)$  given at the beginning of this appendix, by replacing  $\varphi$  with  $W$ . The other von Karman equation is found by combining equations (A20) and (A19):

$$D \nabla^4 W = L(W, \varphi) \qquad (A22)$$

Equations (A21) and (A22) are the von Karman equations and the operators, which are given in rectangular cartesian coordinates at the start of this appendix, can be transformed into polar coordinates using simple coordinate transformations. Since these equations are based on the Lagrangian description, the boundary conditions should be written in terms of the undeformed coordinates. In most of the large deflection plate problems considered previous to this investigation, there is no difference between the Eulerian and Lagrangian type boundary conditions. However, in this problem where the inner boundary is displaced and rotated relative to the outer boundary, the two descriptions are different at  $O(\alpha^3)$ . The boundary conditions and numerical results reported in this work are based on the Lagrangian description, but as a matter of

interest numerical results were also obtained based on Eulerian boundary conditions.

The Eulerian boundary conditions to  $O(\alpha^3)$  can be found from the Lagrangian boundary conditions by substituting  $\sin \alpha$  for  $\tan \alpha$  in equations (30) and (31). The only effect this substitution has on the development in Chapter IV is that the leading terms in the expressions for the constants  $R_{32}$  and  $R_{34}$  in equations (75) are now  $-\lambda^{-2}/36(1-\nu^2)$  instead of  $\lambda^{-2}/72(1-\nu^2)$ . This small change was found to have a negligible effect on the lateral displacement and bending stresses (less than 1/2 of 1 percent), because the angle of rotation is small and also because of the  $\lambda^{-2}$  factor involved.

UNSYMMETRICAL LARGE DEFLECTIONS OF  
AN ANNULAR PLATE

by

William Edmund Alzheimer

ABSTRACT

While solutions to the nonlinear von Karman equations for large deflections of thin plates have been presented for annular plates under certain axisymmetric loading conditions, little work has been done with unsymmetrical large deflections. In this investigation a systematic mathematical iteration technique is used to obtain a solution to the von Karman equations for an annulus fixed at the outer edge and which has a central rigid plug that is rotated about its diameter out of the plane of the plate.

The linear, small-deflection solution to this problem presented by H. Reissner is used as the first approximation for large deflections. By using Reissner's solution for the lateral displacement to evaluate the nonlinear terms in one of the von Karman equations, a linear fourth order partial differential equation for the stress function is obtained. The particular solution to the stress function equation leads to multi-valued in-plane displacements, which are eliminated by proper selection of the homogeneous solution. The boundary conditions

for the stress function equation are written in terms of the in-plane displacements, and wherever trigonometric functions of the small angle of rotation of the rigid inclusion appear, they are expressed in a power series of the angle and terms of higher order than the second power are neglected.

By using the resulting stress function and the Reissner solution for lateral displacement to evaluate the nonlinear terms in the second von Karman equation, a linear, fourth order partial differential equation for the second approximation to the large deflection lateral displacement is obtained. Again the boundary conditions are expressed in a power series of the rotation angle and terms of higher order than the third power are neglected. The solution for the lateral displacement is a function of the first and third powers of the angle of rotation, where the part containing the first power is the Reissner solution and the part containing the third power is a correction term reflecting a reduction in lateral displacement caused by the in-plane stresses. Thus by neglecting the third power of the small angle of rotation, the large-deflection solution reduces to the linear, small-deflection solution.

Any further iterations are not performed because the algebra involved becomes excessive; however, the iteration procedure can be repeated to obtain higher approximations. By taking appropriate derivatives of the stress function and the lateral displacement,

expressions for the bending and membrane stresses as functions of the position in the plate and the angle of rotation are obtained. Numerical results are presented in graphical form for typical plates.

Experimental data was obtained with an 18 inch outer diameter, 7.2 inch inner diameter, 0.0634 inch thick plate made of 7075-T6 aluminum. The results of the iteration solution are found to agree very well with the experimental data for lateral displacements up to one and one-half times the thickness of the plate, but the iteration solution begins to overestimate the nonlinear effect for larger displacements.

As a limiting case to the title problem, an iteration solution for large deflections of a clamped circular plate loaded by a central concentrated moment is given.